Doctoral Dissertations and Master's Theses

Spring 4-2016

Forecast Verification of the Current Icing Potential (CIP) to Predict Lightning Hazards at U.S. Spaceports

Robert Edward Haley
Embry-Riddle Aeronautical University

Follow this and additional works at: https://commons.erau.edu/edt

Part of the Aviation Commons, and the Meteorology Commons

FORECAST VERIFICATION OF THE CURRENT ICING POTENTIAL (CIP) TO
PREDICT LIGHTNING HAZARDS AT U.S. SPACEPORTS

by

Robert Edward Haley

A Thesis Submitted to the College of Aviation, Department of Graduate Studies,
in Partial Fulfillment of the Requirements for the Degree of
Master of Science in Aeronautics

Embry-Riddle Aeronautical University
Daytona Beach, Florida
April 2016

FORECAST VERIFICATION OF THE CURRENT ICING POTENTIAL (CIP) TO PREDICT LIGHTNING HAZARDS AT U.S. SPACEPORTS

by

Robert Edward Haley

This Thesis was prepared under the direction of the candidate's Thesis Committee Chair, Dr. Christopher G. Herbster, Associate Professor, Daytona Beach Campus, and Thesis Committee Members Dr. John M. Lanicci, Professor, Daytona Beach Campus, and Dr. Fredrick R. Mosher, Associate Professor, Daytona Beach Campus, and has been approved by the Thesis Committee. It was submitted to the Department of Graduate Studies in partial fulfillment of the requirements for the degree of Master of Science in Aeronautics
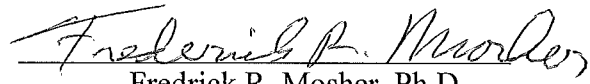
Thesis Committee:

_____
Christopher G. Herbster, Ph.D.
Committee Chair

_____
John M. Lanicci, Ph.D.
Committee Member
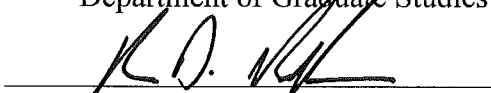
_____
Fredrick R. Mosher, Ph.D.
Committee Member
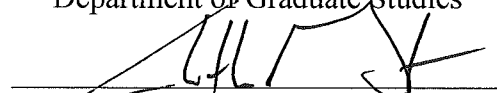
_____
Donald S. Metscher, D.B.A.
Graduate Program Chair
Department of Graduate Studies

_____
Alan J. Stolzer, Ph.D.
Chair
Department of Graduate Studies

_____
Nickolas D. Macchiarella, Ph.D.
Dean, College of Aviation

_____
Christopher D. Grant, Ph.D.
Vice Chancellor of Academic Support

5/2/16
Date

ii

Acknowledgements

I have many people to thank for their help, guidance, and perseverance. I would like to thank Dr. Christopher Herbster for being a mentor through my entire college career with much insight, support, and no direct lightning strikes when sailing near thunderstorms. I also want to thank Dr. John Lanicci for finding the funding that allowed me to pursue my research, and his patience as I learned how to conduct professional research. Finally, I would like to thank my family, especially my Mom and Dad, for doing whatever they could to support me.

Abstract

Researcher: Robert Edward Haley

Title: Forecast Verification of the Current Icing Potential (CIP) to Predict

              Lightning Hazards at U.S. Commercial Spaceports

Institution: Embry-Riddle Aeronautical University

Degree: Master of Science in Aeronautics

Year: 2016

Government spaceports employ extensive lightning detection networks that may not be available at commercial spaceports. Therefore, the Federal Aviation Administration identified the need for diagnosing the threat of triggered lightning without in-situ measurements. Anecdotal observations of the Aviation Weather Center's Current Icing Potential (CIP) diagnostic model indicated a potentially high correlation between lightning activity and icing potential. A forecast verification study and supporting representative case studies were conducted to quantify the CIP's ability to diagnose existing lightning hazards. The study showed that high positive statistical correlations between the CIP and lightning activity do exist, but so do negative correlations. During the forecast verification study, the CIP's ability to diagnose lightning hazards was found to be ineffective due to extensive over-prediction, and, perhaps more importantly, a failure to capture both lightning initiation and cessation. Case study analysis confirmed the CIP's inability to capture lightning initiation and cessation.

Table of Contents

List of Tables

List of Figures

Figure

Chapter I

Introduction

As the United States commercial spaceflight program grows in support of both federal and commercial demands, and the number of licensed and planned spaceports increases, the need exists for a number of weather analysis and prediction tools to support operations. Among these is a tool to provide a regional assessment of the potential of lightning, to include triggered lightning, for planning and safety assessment at these new spaceports. Triggered lightning events involving the damage or destruction of launch vehicles have occurred in the past, the most notable being Apollo 12 on November 14, 1969, and an unmanned Atlas/Centaur rocket on March 26, 1987. In both cases, the vehicles launched through weak cold fronts that were not producing natural lightning, but triggered an electrical discharge between the upper charge region, the vehicle, the vehicle's plume, and the ground. Apollo 12 was able to overcome system failures to complete its mission safely with no harm to its crew. The Atlas/Centaur 67 experienced a system failure that resulted in the loss of the vehicle and payload (Uman & Rakov, 2003).

Significance of the Study

Current government spaceports such as Cape Canaveral Air Force Station (CCAFS), Florida, and Vandenberg Air Force Base (VBG), California, have extensive sensor networks for analyzing the precise conditions of the atmosphere around their facilities and ranges. Because of the lightning hazard in Florida, CCAFS has three separate sensor networks for detecting cloud-to-cloud lightning, cloud-to-ground lightning, and electrical charge in the boundary layer via field mills. At the time this study was conducted, the Federal Aviation Administration (FAA) was uncertain what

types of weather detection equipment and data, if any, commercial spaceports might have (K. Shelton-Mur, personal communication, 2010). To address the threat of lightning at spaceports without in-situ measurements from devices such as field mills, the Current Icing Potential (CIP) weather model, already generated by the National Weather Service (NWS), was evaluated to determine if it could be used to forecast the lightning threat.

Statement of the Problem

There are a number of operational forecast products already in use to diagnose areas of aviation hazards associated with convective activity. Among these is the CIP weather model. The CIP is an operational weather forecast tool that assesses the probability of supercooled liquid water in the atmosphere, which is conducive to structural aircraft icing (Bernstein et al., 2005). In thunderstorms, supercooled liquid water in proximity to an updraft promotes graupel formation; this coexistence of water in solid and liquid forms is known as a mixed-phase environment. Mixed-phase environments generate the charge separation in thunderstorms that produces lightning. Previous research conducted by the FAA and its contractors indicated that occurrences of lightning were highly correlated with the CIP at Spaceport America, Oklahoma Spaceport, Mojave Air and Spaceport, and West Texas Launch Site, analyzed over four years (Shelton-Mur & Walterscheid, 2010). Figures 1 and 2 were presented as evidence of this correlation.
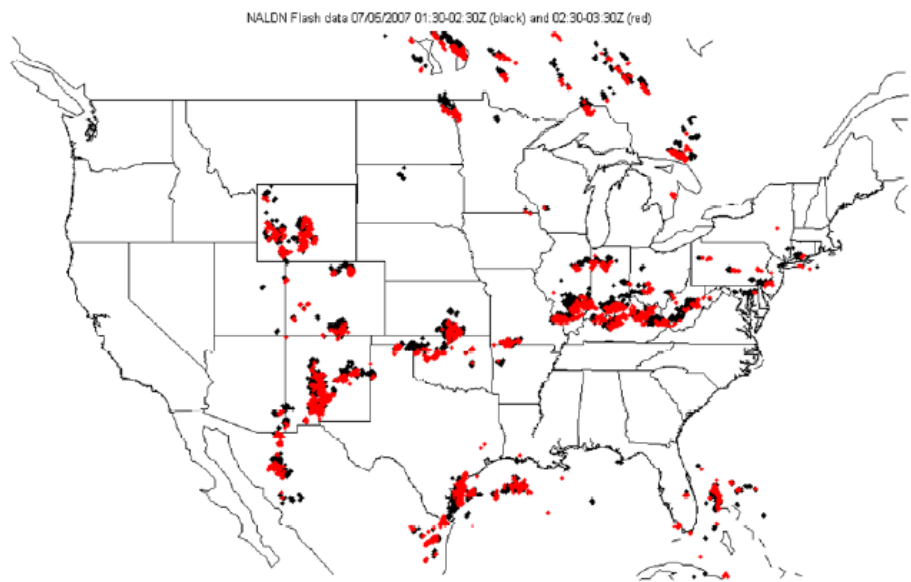
Figure 1. Cloud-to-ground lightning flashes across the U.S. on July 5, 2007. Red marks are flashes between 1:30 UTC and 2:30 UTC. Black marks are flashes between 2:30 UTC and 3:30 UTC (Shelton-Mur & Walterscheid, 2010).
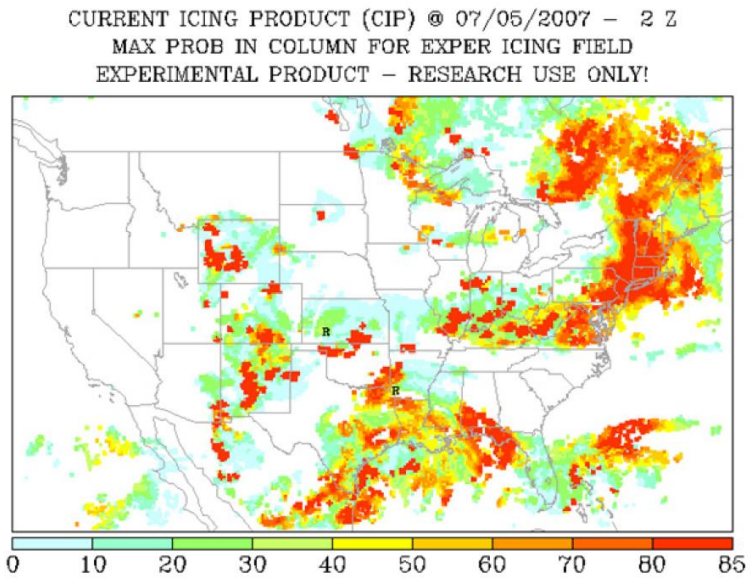
Figure 2. Maximum CIP probabilities across the U.S. on July 5, 2007 (Shelton-Mur & Walterscheid, 2010).

Purpose Statement

The original purpose of this research was to assess the CIP's ability to diagnose triggered lightning hazards from January 2009 until December 2011. Early in the study, the purpose was modified to include assessing *all* lightning hazards due to the limited number of cases where a launch vehicle and its plume triggered a lightning strike. Research on triggered lightning is primarily conducted by firing rockets trailing conductive wires near well-developed thunderstorms (Newman et al., 1967). These conditions are easily recognized as hazardous to launch operations, compared to the marginal conditions that triggered lightning strikes on Apollo 12 and Atlas/Centaur 67. Other triggered lightning research has been conducted using fixed-wing aircraft (Uman & Rakov, 2003).

The final purpose of this study was to determine if the CIP could be used to diagnose the threat from (observed) lightning at commercial spaceports. The researcher determined via statistical analysis and forecast verification whether the CIP could be used to diagnose the threat from (observed) lightning at commercial spaceports as an alternative to on-site detection equipment from field mills.

Research Questions

1. What is the nature of the observed lightning and CIP correlation?
2. Does the CIP have skill predicting lightning at commercial spaceports?

Delimitations

In December 2010, the National Centers for Environmental Prediction (NCEP) released an update to the CIP. This update changed the way model levels were handled, and the change was incompatible with the software scripts developed for this analysis.

The decision was made that the 23 months of collected CIP data starting in January 2009 and running until December 2010 was a sufficient analysis period. No CIP analysis was performed for 2011, but lightning analysis was still done.

Limitations and Assumptions

Limitations in the lightning data occurred in both time and space. The lightning data set contained 1,075 out of 1,095 days over the three-year period. The 20 missing days are likely due to technical issues. In addition, the lightning data set as well as the CIP only covers the continental U.S. (CONUS), and as a result, any launch facilities outside this region, such as those in Alaska, Hawaii, or the Pacific Ocean, could not be included.

Lightning data packets are received every minute by Embry-Riddle Aeronautical University (ERAU). These reports contain all lightning events since the previous data block, or minute, before it. This gives the lightning data a high degree of temporal resolution, even more so than that of radar. Additionally, the locations of the lightning strokes have a very high spatial specificity, with coordinates reported to six or seven decimal places of a degree (Unidata, n.d.). The CIP data to which we intended to correlate the lightning data are updated hourly, which is very rapid by Numerical Weather Prediction (NWP) standards, but results in 60 lightning data blocks for each hourly CIP analysis. This required a scheme to be developed that would generate an hourly lightning data set that would match the CIP temporal domain. The lightning data were processed into an hourly gridded data set with all times from 30 minutes (XX:30) before the hour to 29 minutes (YY:29) after the hour contained in a single file. This file was assigned a valid time on the hour (:00).

The primary literature source for information on the location and license status of spaceports is the FAA's *U.S. Commercial Space Transportation Developments and Concepts: Vehicles, Technologies, and Spaceports*. The latest available version of this document is January 2011.

Definitions of Terms

GRIB File	A binary file whose format is standardized by the World Meteorological Organization and is used for the storage and exchanged of gridded fields (NOAA, n.d.)
Lightning Flash	An entire lightning discharge, including the initial stroke and all return strokes (Uman, 2001).
Lightning Stroke	The individual discharges that make up a lightning flash (Uman, 2001).
T-Storm Day	Any day where at least one lighting stroke was observed (Author).
00:00 UTC	Time reported in Universal Coordinated Time, also known as Greenwich Mean Time (or "Zulu" Time) (USNO, 2016).

List of Acronyms

AMU	Applied Meteorology Unit
BAK	Spaceport Indiana
CASP	California Spaceport
CCAFS	Cape Canaveral Air Force Station
CCS	Cape Canaveral Spaceport
CIP	Current Icing Potential

CONUS	Continental U.S.
CPC	Climate Prediction Center
CSI	Critical Success Index
CSM	Oklahoma Spaceport
EDW	Edwards Air Force Base
ERAU	Embry-Riddle Aeronautical University
FAA	Federal Aviation Administration
FAR	False Alarm Rate
GIS	Geographical Information Systems
GOES	Geostationary Operational Environmental Satellite
GRIB	Gridded Binary (Data)
HRRR	High Resolution Rapid Refresh
IDV	(Unidata) Integrated Data Viewer
KSC	Kennedy Space Center
MARS	Mid-Atlantic Regional Spaceport
MHV	Mojave Air and Space Port
NCAR	National Center for Atmospheric Research
NCEP	National Centers for Environmental Prediction
NCL	NCAR Command Language
NEXRAD	Next Generation Weather Radar WSR-88D Doppler Radar
NLDN	National Lightning Data Network
NOAA	National Oceanic and Atmospheric Administration
NOMADS	NOAA/National Model Archive and Distribution System

NWP	Numerical Weather Prediction
NWS	National Weather Service
POD	Probability of Detection
POES	Polar Operational Environmental Satellite
RAP	Rapid Refresh
RUC	Rapid Update Cycle
SPAM	Spaceport America
SPC	Storm Prediction Center
SR	Success Ratio
TDWR	Terminal Doppler Weather Radar
UCAR	University Corporation for Atmospheric Research
U.S.	United States
USNO	U.S. Naval Observatory
UPSLN	United States Precision Lightning Network
UTC	Universal Coordinated Time
VBG	Vandenberg Air Force Base
WFF	Wallops Flight Facility
WSMR	White Sands Missile Range
WSR-88D	Weather Surveillance Radar 1988 Doppler

Chapter II

Review of the Relevant Literature

Topics covered for the literature review include weather modeling, lightning formation and forecasting, triggered lightning research and incidents, and the spaceports analyzed in the study.

Weather Modeling of Supercooled Liquid Water

Current Icing Potential. The CIP is an algorithm that uses observations from satellite, radar, surface observing stations, lightning, and pilot reports, with NWP to diagnose the potential for icing and supercooled liquid water (Bernstein et al., 2005). The CIP was developed to forecast short-term icing conditions for the FAA. The output is produced hourly in a three-dimensional domain using methods developed from field programs and cloud physics principles.

Historically, aircraft icing was forecast manually using a limited set of fields such as relative humidity, temperature, and vertical motion. The CIP utilizes these as well as other techniques to create a more complete picture, and diagnose the potential for icing in different environments. The data sets are applied to the Rapid Update Cycle (RUC) model grid (note: in May 2012, the RUC was replaced by the Rapid Refresh [RAP] model [NOAA, 2015]). The three-dimensional location of clouds and precipitation is then determined by observations from sources such as satellite and radar. Next, the fuzzy-logic functions are performed, and then a decision tree is utilized. Fuzzy-logic better handles function uncertainties by assigning values from zero to one rather than absolute Booleans or thresholds (Bernstein et al., 2005). The decision tree is then used to determine the physical icing situation. The icing situations are a single-layer cloud,

multiple-layer clouds, cloud-top temperature gradients, freezing rain, and deep

convection (Bernstein et al., 2005). The final icing potential is then calculated by

boosting the factors up or down. An upward boost is given to initial icing potential areas

where icing is reported, or model upward vertical motion and/or model supercooled

liquid water is forecast. Only model forecasts of downward vertical motion can decrease

the icing potential. Bernstein et al. (2005) presented four case studies of CIP

performance in a single-layer cloud, freezing rain, cloud-top temperature gradient, and a

poorly handled single-layer cloud. The statistical performance of the CIP against pilot

reports of icing is also presented, where the CIP is shown to have a high degree of

accuracy.

Rapid Update Cycle. The RUC was an operational NWP model used by NCEP

(Benjamin et al., 2004a). The RUC supplemented longer-range, less frequently updated

NWP models by using a shorter update cycle (~ 1 hour) to achieve a more accurate short-

range model forecast. A shorter-range model with a faster update cycle has applications

for fields sensitive to quickly changing weather conditions, such as thunderstorms and

icing, which are of particular interest to aviation. At the time of this study, the

operational RUC used a 20 km (kilometer) horizontal grid with a 1-hour update cycle and

50 vertical levels using a hybrid sigma-isentropic vertical coordinate. The domain

covered the CONUS, as well as adjacent Canada, Mexico, and the Atlantic and Pacific

Oceans. Observational data for the RUC came from high-frequency sources to facilitate

the 1-hour cycle; thus, the data assimilation scheme had to overcome significant

challenges in order to remain numerically stable, with spurious gravity waves and

aliasing being a particular issue (Benjamin et al., 2004a). A noise-control process

controlled the gravity waves, while observation-time windows selected the data used for assimilation. The high frequency data sets and the quick update cycle of the RUC worked well to maintain temporal stability, but the asynchronous and irregularly spaced aircraft observations, one of the RUC's more important data sources, led to the aforementioned aliasing issues as their spatial and temporal resolution is inconsistent (Benjamin et al., 2004a). Despite the challenges of data assimilation, the RUC has been statistically proven more accurate in short-range forecasts than long-range NWP models and short-range persistence, with the exception of a few fields (Benjamin et al., 2004a). At the conclusion of this study, the RUC had been replaced by the Rapid Refresh (RAP) model, which was in turn complemented by the High Resolution Rapid Refresh (HRRR) model (NOAA, 2015).

Lightning Formation

The fundamental cause of lightning formation is separated electrical charge regions in clouds and/or the ground, which are strong enough to create a channel for electrons to flow through. The lightning discharge is usually comprised of multiple individual strokes, with the entire event being called a flash. Martin A. Uman did much of the work to understand lightning formation, from which two books are used to explore lightning basics and then a more detailed analysis of the discharge.

In the book *Lightning*, Uman (2011) presents basic knowledge of lightning formation and the different types of commonly observed lightning discharges. These discharges can be grouped into three general categories based on the characteristics of formation: (a) negative cloud-to-ground, (b) positive cloud-to-ground, and (c) cloud-to-cloud. A negative cloud-to-ground discharge occurs when charge separation between the

ground and clouds results in the flow of electrons from the positively charged ground to the negatively charged cloud. A positive cloud-to-ground stroke discharge is similar to a negative cloud-to-ground discharge, but the electrons flow from the positively charged cloud to the negatively charged ground. A cloud-to-cloud discharge is the flow of electrons from a cloud or region with positive charge to a cloud or region with a negative charge, never contacting the ground.

The specific characteristics of the different lightning polarities were detailed in *The Lightning Discharge* (Uman, 2001). Negatively charged lightning is produced when an electrical channel is established from the negatively charged lower regions of the cloud with the positively charged ground, resulting in the transport of electrons from the surface to the cloud visibly seen as cloud-to-ground, or forked, lighting. Positively charged lightning events occur with the opposite current flow, often when upper-level clouds from a thunderstorm are transported downwind ahead of the storm carrying a positive charge in the cloud and inducing a negative charge at the surface. When an electrical channel is established, electrons flow from the cloud to the surface. This positive discharge is approximately three times stronger and five times slower than that of a negative charge. The positive stroke poses a particularly dangerous hazard to safety since it can strike "out of the blue" from the anvil or other high parts of the cloud miles away from the active part of the thunderstorm, with a much greater charge and exposure period than that of negatively charged lightning. Cloud-to-cloud lightning is produced when oppositely charged regions of clouds establish an electrical channel resulting in a discharge between clouds or within parts of a cloud. This discharge strength and duration is approximately equivalent to a negative cloud-to-ground stroke (Uman., 2001).

Triggered lightning is an event where a disturbance helps create a channel between the separated electric fields promoting the flow of electrons. This produces a lightning discharge that might not have occurred naturally.

Lightning Forecasting

Numerous studies in lightning forecasting have been conducted by the NWS, universities, and the Applied Meteorology Unit (AMU) at CCAFS. The methods used or examined include statistical algorithms, radar signature analysis, stability index algorithms, model parameter algorithms, and combinations of all or some of these.

Many subsequent publications in this literature review reference Reap (1986), who analyzed synoptic patterns and the subsequent low-level wind flow regimes. At the time of the publication, the goal was to present some type of system for forecasting the timing and intensity of deadly cloud-to-ground lightning. Using different map types and different flow regimes, Reap was able to develop the concepts used in many of the papers that relate the known lightning hotspots to the type of synoptic conditions that promote them (Reap, 1986).

The AMU at CCAFS used information gathered from two previous research projects and fifteen years (1989-2003) of warm season weather data to develop forecast equations for determining the probability of lightning hazards during the Florida warm season (May-September). The previous studies determined logistic regression outperformed previous lightning forecasting methods. The warm season data sources included cloud-to-ground lightning for determining lightning occurrences, Florida synoptic soundings for calculating flow regimes, and CCAFS soundings for calculating local stability parameters. The flow regime and stability parameters provided 13

candidate predictors for equations development. One equation was developed for each warm season month, with differing predictors in the equations that best capture the progression of lightning activity through the Florida warm season. These equations are used in daily and weekly planning forecasts for general scheduling and in support of launch operations (AMU, 2005).

The Storm Prediction Center's (SPC) efforts to forecast lightning, detailed by Bothwell (2009), started in the early 2000s with the intent to forecast dry lightning strikes in support of fire-weather forecasting. These efforts used lightning climatology and NWP model predictor fields to create a "perfect prognosis" forecast for lightning. The perfect prognosis assumes the NWP model is "perfect" and looks for conditions based on lightning climatology that have been statistically proven precursors to lightning activity. The output is created by applying equations to nearly 200 predictor fields in any model, long and short range, providing the perfect prognosis forecast out to the length of the forecast model run. Over the years, the forecast system has been modified to include Alaska and other non-CONUS areas as well as forecast excessive lightning events in addition to dry lightning events (Bothwell, 2009).

Shafer and Fuelberg (2006) used 16 warm seasons of National Lightning Data Network (NLDN) and radiosonde-derived parameters to produce statistical lightning guidance equations for predicting warm season, afternoon-to-evening lightning onset for the Florida Power and Light Company in 11 Florida counties. The most dominant predictor in the guidance equations was prevailing low-level winds, with the K index, Showalter index, previous day lightning persistence, and morning lightning also being important predictors. Using these predictors, the guidance equations showed significant

improvement over persistence forecasts. However, the guidance equations were dependent on morning soundings being representative of large parts of Florida for the entire day. As a result, days when atmospheric conditions changed across the forecast area or throughout the day (such as a new air mass advecting into the area) resulted in errors in the lightning forecast (Shafer & Fuelberg, 2006).

Shafer and Fuelberg (2008) used NWP and the perfect prognosis method to overcome the drawbacks of the guidance forecast equations developed in Shafer and Fuelberg (2006), with the main objective being the development of high-resolution gridded guidance for warm-season cloud-to-ground lightning. The perfect prognosis method produced positive skill using three different NWP models and concluded that skillful lightning forecasts out to 6-9 hours are possible with high-resolution models; skill was consistent enough between models to conclude the perfect prognosis method worked well independent of model type. Forecast accuracy decreased past 9 hours (Shafer & Fuelberg, 2008).

Current lightning and electrical field detection technologies are inadequate for predicting hazards at large scales. Lightning detection networks have long detection ranges but have no predictive ability, while field mills can provide an assessment of the potential for lightning but their ranges are limited to 20 km or so (Murphy, Holle, & Demetriades, 2008). Therefore, many studies have been done to find radar signatures that would pre-empt the first strike and even allow for warnings. Gremillion and Orville (1999) investigated numerous warm-season air mass thunderstorms around the KSC from 1992 to 1997 utilizing the NWS's Weather Surveillance Radar 1988 Doppler (WSR-88D) in Melbourne, Florida, as well as the NLDN. Previous studies had indicated that charge

separation occurred in storms with updrafts strong enough to reach the -10 to -15 degree

Celsius height where liquid and solid water were interacting. Using this as a baseline,

they compared radar volume scans with lightning data to find that radar signatures of 40

decibels at the -10 degrees Celsius height can be used to predict the onset of lightning.

The study conducted by Hondl and Eilts (1994) is very similar to that of

Gremillion and Orville, though Hondl and Eilts' study was published several years

before. Once again, radar signatures were correlated with NLDN data to find signatures

that would help indicate the onset of lightning. Radar data from the FAA Terminal

Doppler Weather Radar (TDWR) in Orlando, Florida, was used, as well as data from the

WSR-88D in Melbourne.

Triggered Lightning Strikes on Aircraft and Spacecraft

Triggered lightning has been investigated by four instrumented aircraft, as well as

in two incidents where video was captured of commercial airliners triggering lightning

strikes. These incidents, as well as Apollo 12 and Atlas/Centaur 67, were investigated by

Uman and Rakov (2003). In four separate studies, instrumented aircraft were

intentionally flown into and around thunderstorms in Florida (Fitzgerald, 1967), Virginia

(Pitts, Fisher, Mazur, & Perala, 1988), France (Moreau, Alliot, & Mazur, 1992), and

again in Florida (Rustan, 1986), to understand the aircraft's role in triggering lightning

strikes. These studies, plus data available on lightning strike accidents involving

commercial aircraft, support the conclusion that 90% of lightning strikes on aircraft and

spacecraft are triggered by the craft itself. This conclusion is supported by radar analysis

of a National Aeronautics and Space Administration (NASA) F-106B research aircraft,

where UHF radar echoes showed that the initial lightning leader channels originated at or

near the aircraft and propagated away from it (Uman & Rakov, 2003). Additional

support for the aircraft-initiation hypothesis is provided by analysis of electrical field

waveforms on the surface of a CV-580 research aircraft (Uman & Rakov, 2003) and

multipoint electric field measurements on a French C-160 aircraft (Moreau et al., 1992).

Due to the strict weather launch criteria at current spaceports, the occurrences of

triggered lightning strikes on spacecraft are rare. The two most notable lightning strikes

on spacecraft were Apollo 12 in 1969 and an unmanned Atlas/Centaur in 1987, the latter

serving as a reminder of the catastrophic loss a lightning strike can cause.

Apollo 12. Uman and Rakov (2003) analyzed the lightning strike triggered by

Apollo 12 in 1969 at Kennedy Space Center (KSC) in Florida. The conditions were

similar to that of Atlas/Centaur 67, though less is known about the environment due to

the primitive operational weather sensing equipment in 1969. A weak cold front was in

the proximity of KSC, with no lightning reported within six hours of launch by the

lightning detection equipment available at the time (Uman & Rakov, 2003). Shortly after

launch, the vehicle triggered two separate discharges that damaged and disrupted

spacecraft systems. Unlike Atlas/Centaur 67, Apollo 12 was able to overcome the system

upsets to reach orbit safely and complete its mission.

Atlas/Centaur 67. Christian et al. (1989) detailed the atmospheric conditions that

produced the Atlas/Centaur 67 triggered lightning strike at CCAFS, as well as the

sequence of events. As with Apollo 12, a weak front, in this case a nearly stationary cold

front, extended across Florida from southwest to northeast across the panhandle. The

strongest convection associated with the front was being produced in a squall line that

crossed the Florida panhandle into the Gulf of Mexico.   This squall line was well north

of Cape Canaveral at the time of the lightning strike. Conditions at the launch site were described (after the fact) as weakly convective with thunderstorms in the area "in the broadest sense of the word" (Christian et al., 1989). There was occasional lightning, dark clouds, and strong precipitation on the ground. No cloud-to-ground lightning was detected within five nautical miles of the launch site in the 42 minutes prior to the launch, though an undetected cloud discharge was observed by press two minutes prior to launch. Forty-nine seconds after launch there was a lightning flash observed below the cloud base. The vehicle was inside a cloud at an altitude of 12,000 feet where the temperature was 4 degrees Celsius, 2,400 feet below the freezing level (14,400 feet). The radar echo within the cloud was only 10 decibels, considerably lower than the 40 decibels of cumulonimbi in the area. The lightning strike caused a memory error that made the vehicle's computer issue a hard over engine gimbal command, increasing the angle of attack and generating excessive aerodynamic loads that resulted in the destruction of the launch vehicle and payload (Christian et al., 1989).

Spaceports for this Study

The following is a brief summary of the spaceports selected for this study. For the most part, only FAA-licensed commercial spaceports were selected (FAA, 2011). For most of the following locations, there is a broad area that defines the spaceport; for this study, a central latitude and longitude were selected to define the area to be included in the analysis. In all cases, this area was defined in equidistant Cartesian coordinates, regardless of the shape of the actual spaceport domain.

California Spaceport. Located at 34.58 degrees north latitude and 120.63 degrees west longitude on the California coastline, California Spaceport (CASP) is the

westernmost launch facility within the CONUS. Operated by Spaceport Systems International, CASP was the first spaceport to receive an FAA Commercial Space Launch Site Operator's License, which was issued in 1996. It utilizes Space Launch Complex-8 at Vandenberg Air Force Base (VBG), part of the Western Test Range. The Western Range supports orbital and suborbital flights from the west coast, and launches from this complex are generally destined for polar orbits (Spaceport Systems International, n.d.).

Cape Canaveral Spaceport. Located at an estimated position of 28.46 degrees north latitude and 80.53 degrees west longitude on the Florida east coast, Cape Canaveral Spaceport (CCS) is one of the southernmost launch facilities within the CONUS. Operated by Space Florida and co-located with CCAFS and KSC, CCS utilizes Launch Complexes LC-36, LC-46, and LC-47. CCS also supports Space Exploration Technologies (SpaceX) launches at LC-40. Space Florida obtained an FAA Commercial Space Launch Site Operator's License for LC-46 in 2010, and currently operates LC-36 under the Air Force's Real Property License (FAA, 2011). CCS, CCAFS, and KSC are all within 20 km of each other, meaning they would either all be in the same model grid square, or at most, adjacent grid squares, and individual analysis would unnecessary duplicative effort, with results that would have no statistical independence. CCS will be used to identify CCS/CCAFS/KSC because of this study's focus on commercial spaceports.

Mid-Atlantic Regional Spaceport. Mid-Atlantic Regional Spaceport (MARS) is located at 37.83 degrees north latitude and 75.49 degrees west longitude on the Virginia coastline, making it, and Wallops Flight Facility (WFF), the easternmost launch facilities

in the CONUS. The Virginia Commercial Space Flight Authority received a Space Launch Site Operator's License in 1997 for a spaceport co-located at WFF. MARS operates launch pads 0-A and 0-B. While WFF mainly specializes in suborbital and balloon launches, MARS has developed facilities to support resupply missions to the International Space Station in low Earth orbit was well as lunar probes (FAA, 2011).

Mojave Air and Spaceport. Mojave Air and Spaceport is located at approximately 35.06 degrees north latitude and 118.15 degrees west longitude in California. This spaceport is operated by East Kern Airport District and home to Masten Space Systems. As of January 2011, Mojave Air and Spaceport was not yet licensed by the FAA to conduct commercial vertical launches, but has the facilities to conduct vertical launch tests. Masten uses the facilities to design, build, and test reusable vertical take-off and landing vehicles for NASA contracts, as well as other vehicles such as The Spaceship Company's WhiteKnightTwo and SpaceShipTwo. Other companies use the current and upgrading facilities, including large runways, to test vertical and horizontal take-off vehicles (FAA, 2011).

Oklahoma Spaceport. Oklahoma Spaceport is located at approximately 35.34 degrees north latitude and 99.20 degrees west longitude; this spaceport is one of the few in the central U.S., where coastal zones or expansive deserts are not available for use as ranges. Operated by the Oklahoma Space and Industry Development Authority, this spaceport utilizes a large runway and other facilities to support horizontally launched suborbital vehicles (FAA, 2011).

Spaceport America. Spaceport America is located at approximately 32.99 degrees north latitude and 106.97 degrees west longitude in New Mexico. Operated by

the New Mexico Spaceport Authority, Spaceport America is the world's first purposely built commercial spaceport currently capable of supporting vertical and horizontal suborbital launches. Spaceport America's proximity to the White Sands Missile Range to the east allows use of that range for launch and recovery operations. The spaceport has been used by commercial and government contractors for test flights. However, it will most notably facilitate Virgin Galactic's WhiteKnightTwo aircraft and SpaceShipTwo spacecraft (FAA, 2011).

Spaceport Indiana. Spaceport Indiana is a proposed spaceport co-located at Columbus Municipal Airport near Columbus, Indiana. It is located at approximately 39.26 degrees north latitude and 85.91 degrees west longitude, making it one of a few spaceports not near a coast or military range. In 2010, Spaceport Indiana was limited to education and hobby rocketry, but still has a proposed status as compared to an inactive status (FAA, 2011). .

Summary

Lightning is caused by establishing a channel between separated electrical charge regions in the atmosphere and/or ground. Four studies where test aircraft were intentionally flown in and around thunderstorms have shown aircraft are capable of establishing an electrical channel between charged regions and generating triggered lightning. These tests used UHF radar echoes, analysis of electrical field waveforms, and high-speed video, to confirm lightning channels originated from the aircraft.

Lightning forecasting research has focused on development of model and/or statistical tools for strategic diagnoses (out several hours) and weather radar signatures for tactical diagnoses of imminent lightning activity. These forecasting tools have often

relied on numerous derived and observed parameters applied to specially developed equations to beat persistence and climatology forecasts of lightning hazards. The AMU at CCAFS has spent years developing a lightning probability tool that requires up to thirteen predictors used in forecast equations, one equation for each month of the warm season, at that spaceport. Other studies have followed suite, using many years of data to develop methods for forecasting lightning at relatively constrained locations for specific times of the year. For diagnosing impending lightning threats, studies have shown radar echoes of 40 decibels at the -10 Celsius height can be used to predict the onset of lightning. This description of previous lightning research sets the stage for the present study, which is focused on FAA-approved commercial spaceports.

Chapter III

Methodology

Statistical analysis and forecast verification were the primary methods for addressing the research questions. Analysis and verification were accomplished by retrieving lightning and CIP data, setting the data onto a common grid with an objective technique, and then analyzing the data using National Center for Atmospheric Research Command Language (NCL) scripts.

Lightning Data Selection Criteria

Lightning data networks, unlike most U.S. meteorological information infrastructure, are privately owned. Two major detection networks, the NLDN operated by Vaisala, and the United States Precision Lightning Network (USPLN) operated by Weather Services International (now The Weather Company), provide real-time and archived lightning data to subscribers and recent data on a time-delay to the public. The CIP uses the NLDN as the primary data source for determining the location of deep convection. The USPLN dataset was selected for the analysis in this study for the following reasons: (a) ERAU's involvement with the academic distribution of USPLN provided a sizable lightning data archive; (b) the network's reporting of individual strokes, cloud-to-cloud events, stroke polarity; and, perhaps most important, (c) data independence from the CIP product.

Data Retrieval

Retrieval of the data for this project was straightforward. The Meteorology program at ERAU archives USPLN lightning data internally going back to 2006. CIP

data was retrieved from the National Centers for Environmental Information's NOAA

Operational Model Archive and Distribution (NOMADS) system.

Gridded Lightning Data Set

In order to perform the analysis of the data, lightning events, which occur at point

locations and at specific times, had to be mapped to the CIP grid locations and placed

into temporal bins that best represented the lightning activity for a forecast/analysis hour.

USPLN produces reports every minute containing the date/time, location, polarity, and

other information for all detected lightning events that occurred since the previous data

packet. A solution that used the latitude and longitude of a stroke to determine the CIP

grid box of that lightning event was developed. The assignment of times, also in the

software solution, was more complicated. While the CIP has a relatively high temporal

resolution (1 hour) for an NWP-based system, lightning events occur rapidly with

hundreds and even thousands of strokes during the same period. The lightning data

needed to be set to hourly time intervals, but this created fundamental issues concerning

which hour a lightning stroke is valid. Two options were available: (a) use bins starting

on the hour where all stroke events from XX:00 UTC to XX:59 UTC are valid at XX:00

UTC, or (b) centered on the hour where all strokes from XX:30 UTC to XY:29 UTC (the

next hour) are considered valid at XY:00 UTC. Though more complicated to process, the

latter solution was selected, as centering on the hour ensured none of the lightning data's

time stamps were off by more than 30 minutes. Using the former scheme, a lightning

strike at 00:59 UTC would have been valid for 59 minutes earlier at 00:00 UTC even

though it occurred one minute before the next hour.

The data were also broken up into three categories based on lightning type reported by the USPLN: (a) negatively charged lightning, (b) positively charged lightning, and (c) cloud-to-cloud lightning. A fourth category totals the three separate lightning types. The partitioning of the strokes is consistent with looking for relationships in the differences among the physical processes producing the lightning stroke.

The gridded stroke events were assembled into hourly Gridded Binary (GRIB) files that matched the analysis/forecast times of the CIP files. Initial analysis of the CIP files with the gridded lightning data proved difficult when working with all the CIP levels. The level that matched lightning activity alternated from 4,000 to 6,000 meters above mean sea level depending on latitude and time of year. With no apparent relationship of lightning activity to the CIP vertical levels, the CIP data were processed to create a single value of the highest CIP value in a column for each grid across all levels, analogous to a composite reflectivity for Next Generation Radar (NEXRAD) data.

Analysis Components of this Study

Exploratory and statistical analysis of the gridded lightning data set are provided at the CONUS level, and regionally around current and proposed spaceports not classified as inactive. These spaceports included CASP, CCS, MARS, MHV, CSM, SPAM, and BAK. These locations were selected based on current or potential commercial launch activity, vertical launch facilities, and previously established lightning climatology for selected locations.

Lightning data analysis. An initial exploratory analysis was performed to provide an assessment of the gridded lightning data set to generate qualitative

information on the differences in lightning activity between spaceports and across the country. Two methods of reading the lightning data were performed. The first method read through the GRIB files for each day of the year to determine the grid box that experienced the maximum lightning event counts for each category. This analysis proved to be a nonproductive effort as the results were not intuitive, with limitations in analyzing when and where these maximums occurred, as well as discontinuities among the four categories. The second method also read through the GRIB files for each day of the year, summed the lightning events for each category at each grid box, and summed all the grid boxes, producing a daily sum of all events for each category across the prescribed region. This method proved very informative as to which days were active, which spaceports were more active than others, along with the seasonality of the lightning activity.

A regional analysis was conducted around CASP, CCS, MARS, MHV, CSM, SPAM, and BAK, by including only lightning events that occurred within five grid boxes north, south, east, and west of the grid box that contains the spaceport. This produces a region of 11 by 11 grid boxes (each grid box is 20 km on a side), or 220 by 220 km, covering an area of 48,480 square km. The location of the spaceport, or in some cases specific launch facilities, was determined via Internet search for these facilities including the use of a Geographical Information System (GIS) such as Google Earth[TM] to identify the location and extent of ground facilities. For companies that only have a single vertical launch facility, the exact coordinates of the tower were retrieved, while launch ranges and airports for horizontal launches used approximations based on a central part of the facility (usually the runway that would be used for launch and recovery). With the exception of very large ranges such as White Sands in New Mexico, any error in the

exact launch point estimation is far less than a 20-km model grid box. Facilities selected

are listed in Table 1. During the analysis, the researcher removed the following co-

located spaceports: KSC/CCAFS (see CCS), WFF (see MARS), VBG (see CASP), EDW

(see MHV), and WSMR (see SPAM).

Table 1

Locations of CONUS Spaceports

	Latitude	Longitude
Kennedy Space Center (KSC)[b]	28.61	80.60
Cape Canaveral Air Force Station (CCAFS)[b]	28.49	80.58
Cape Canaveral Spaceport (CCS) [b]	28.46	80.53
Wallops Flight Facility (WFF)[b]	37.84	75.48
White Sands Missile Range (WSMR)[b]	33.11	106.43
Edwards Air Force Base (EDW)[a]	34.95	117.88
Vandenberg Air Force Base (VBG) [a]	34.67	120.61
Mid-Atlantic Regional Spaceport (MARS)[b]	37.83	75.49
Oklahoma Spaceport (CSM)[a]	35.34	99.20
Spaceport America (SPAM)[c]	32.99	106.97
Mojave Air and Space Port (MHV)[1]	35.06	118.15
California Spaceport (CASP)[c]	34.58	120.63
Space Port Indiana (BAK) [a]	39.26	85.91

[a] Abbreviated identifier used is based on FAA location identifier. These locations are airports or military bases
[b] Abbreviated identifier used is based on officially designated or industry standard conventions
[c] No identifier could be obtained and one was created

In many cases, commercial companies used the existing launch facilities at government spaceports such as CCAFS, VAB, and WFF. Other companies have their own launch facilities built near government ranges to utilize the range safety facilities. For example, SPAM is adjacent to WSMR, and MHV is near EDW. Because of the often-close proximity of the commercial spaceports to government spaceports, many regional domains overlapped. In these circumstances, regional analysis was only done on the commercial spaceport in the commercial-government spaceport pairs.

Some spaceports that are considered inactive were still used to create regularly spaced analysis points across the CONUS.

Statistical correlations. The statistical correlations were performed using software that directly compared the lightning and CIP gridded data sets. Two types of correlations were performed, temporal and spatial.

Horizontal correlations were calculated at each of the CIP's vertical levels (based on the RUC's vertical levels) to investigate whether lightning was forecast better at certain levels than others. Additionally, to overcome our observation that peak vertical correlations were temporally and spatially variable, the use of the "max-CIP" field was implemented. This choice had results that were more favorable than any single level provided. Recall that max-CIP analyzes every model level inside a column to find the maximum value of CIP observed in the column, which produces a single level "worst-case scenario" atmosphere.

Temporal correlations were produced by keeping location (grid box) constant and varying time, while horizontal correlations were produced by keeping time constant and varying location. Correlations were calculated so areas of lightning and CIP would have

high values; meanwhile, areas of CIP and no lightning (false alarms) and areas of

lightning but no CIP (missed events) were not shown, as a zero field has no correlation

with another data set. An example is provided in Figure 3 below.
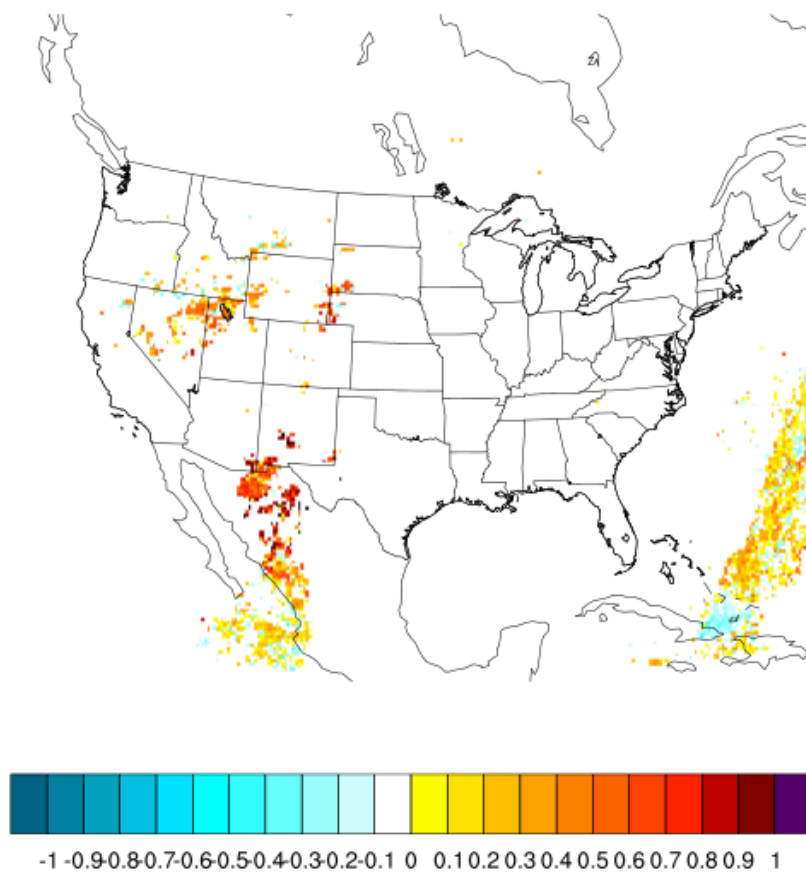
Figure 3. Sample of max-CIP and lightning correlations. Reds indicate positive
correlations and blues negative correlations.

During the correlation analysis, there were numerous instances of negative

correlations. The nature of these occurrences was investigated by manually viewing the

CIP and lightning data together, and negative correlations were found for cases where

lightning occurred without CIP. Because lightning occurring without CIP would defeat the purpose of using the CIP as a lightning diagnostic, specific cases of negative correlations near current and proposed spaceports were selected for further review.

Forecast verification. Three types of forecast verifications were conducted to determine the CIP's ability to forecast lightning. The first used an ERAU database developed to search a weather data archive that focused on aviation hazards, including CIP and precipitation, to find false alarm rates. The second forecast verification was conducted using a contingency table of CIP and lightning. The third forecast verification was also a contingency table, but used lightning persistence instead of CIP to forecast lightning. This persistence verification was done at the same spaceports as the CIP-lightning verification to provide comparison of the CIP's skill to that of the persistence forecast.

CIP – Lightning forecast verification. Contingency tables are a commonly used tool in meteorology to determine the quality of a forecast (Wilks, 2006). The table uses a 2x2 grid to show the outcomes of a forecast-event pair, and the table also provides a way to answer the question, "Was it forecasted, and did it occur?" For this assessment, a CIP probability of 50% was used as the forecast predictor for lightning (i.e., 50% or greater is a forecast for lightning to occur). The contingency table provides measures of "Hit" (H = CIP $\geq$ 50% and lightning occurs), "Miss" (M = CIP < 50% and lightning occurs), "False Alarm" (FA = CIP $\geq$ 50% and lightning does not occur) and "Correct Null Events" (C = CIP < 50% and lightning does not occur). Contingency table results were then used to calculate forecast verification metrics. The metrics selected were Probability of

Detection (POD), Success Ratio (SR), False Alarm Rate (FAR), and Critical Success

Index (CSI).

For general comparison, forecast verification done by NASA's AMU at KSC is

also included. The AMU developed a probabilistic lightning forecast tool to support

operations at CCAFS and KSC, performing the same forecast verification procedure as

this study (AMU, 2005). Forecast verification for the AMU's probabilistic lightning tool

was done on Florida wet seasons prior to 2005 and cannot be directly compared, but the

AMU tool's performance can give an idea of the quality of the CIP's performance.

Persistence forecast of lightning verification. In order to provide a direct

comparison of CIP forecast success, a lightning persistence forecast was created and

verified. The lightning persistence forecast was created for all three years (2009, 2010,

and 2011) using the same scripts and tools for the CIP-lightning forecast verification.

The gridded lightning dataset was used as both observation and forecast in contingency

tables. The same forecast verification metrics (POD, SR, FAR, and CSI) were performed

on the lightning persistence forecast.

Case studies. In-depth analysis of each spaceport is beyond the scope of this

research. Therefore, after the exploratory analysis, three cases were selected for location-

specific studies of the viability of using the CIP to diagnose lightning threats. Cases with

strong and weak correlations were selected to demonstrate how the CIP reacts before and

during the onset of lightning activity. These case studies provide an idea of how well the

CIP would perform in an operational setting.

Chapter IV

Results

Lightning Data Analysis

An exploratory analysis of the gridded lightning data was conducted as an initial

assessment of lightning activity at each of the spaceports as well as across the entire

country. This analysis provided a novel assessment to determine which methods were

nonproductive efforts or provided meaningful qualitative results.

CONUS daily sum event counts. The daily sum event counts provided the sum

of the four categories in each grid box, and then added all the grid boxes to produce a

total number of lighting strokes per day for the entire CONUS.

2009 lightning data review. This year had the lowest total lightning activity of

the three years analyzed, with 52,802,485 total strokes across the CONUS. Table 2

shows information on the distribution of lightning across the CONUS in 2009, using

automatic color-coding, which was applied to some tables in this study[1]. Nearly two-

thirds (63.23%) of lightning activity for the entire year occurred during the summer

months, defined as June, July, and August. The overwhelming majority, 89.66%, of

recorded strokes were negative cloud-to-ground.

Table 3 contains a basic statistical analysis of the four lightning categories for

2009, including how much of the activity occurred during the summer. The maximum

events occurred on the following dates: total and negative were on August 6, 2009,

positive was on July 14, 2009, and cloud-to-cloud was on August 17, 2009. Nearly two-

---

[1] In these tables, each category (column) is a discrete set of results, with thresholds and magnitudes differing from the rest of the categories. Thresholds are based on the maximum and minimum values of each category, with red being the maximum and green being the minimum, with color shading transitioning from red, to orange, to yellow, to green.

thirds of the occurrences (63.23%) were in the summer. The lightning data set is highly

skewed, as shown in Figure 4. The histogram shows that the distribution more closely

matches a gamma distribution than a normal distribution.

Table 2

Monthly Lightning Activity for 2009

	% of Year	All Categories	Negative	Positive	Cloud-to-cloud
Jan	0.21%	108737	102624	1273	4825
Feb	0.80%	421108	384017	6272	30819
Mar	0.49%	259709	226834	4466	28409
Apr	4.87%	2570686	2324368	27347	218971
May	8.95%	4727637	4347936	40045	339656
Jun	17.41%	9192605	8487595	67414	637596
Jul	22.44%	11848109	10799571	269081	779457
Aug	23.38%	12346128	10126014	163829	2056285
Sep	12.13%	6405524	5938166	75825	391533
Oct	5.73%	3025895	2808206	38061	179628
Nov	1.67%	882305	839117	11844	31344
Dec	1.92%	1014042	956299	11846	45897
Summer	63.23%	33386842	29413180	500324	3473338
Total		52802485	47340747	717318	4744420
% of all categories			89.66%	1.36%	8.99%

Table 3

Daily Lightning Statistics for 2009

	All Categories	Negative	Positive	Cloud-to-cloud
Maximum	607461	568095	39157	151717
Third Quartile	263750	224582	2352.5	17168
Mean	150434.4	134873.9	2043.641	13516.87
Median	96372	86033	994	5161
First Quartile	11663	10922.5	160	519.5
Minimum (non-zero)	6	6	1	3
Standard Deviation	155586.7	138354.6	3659.743	22105.8
Interquartile Range	252087	213659.5	2192.5	16648.5
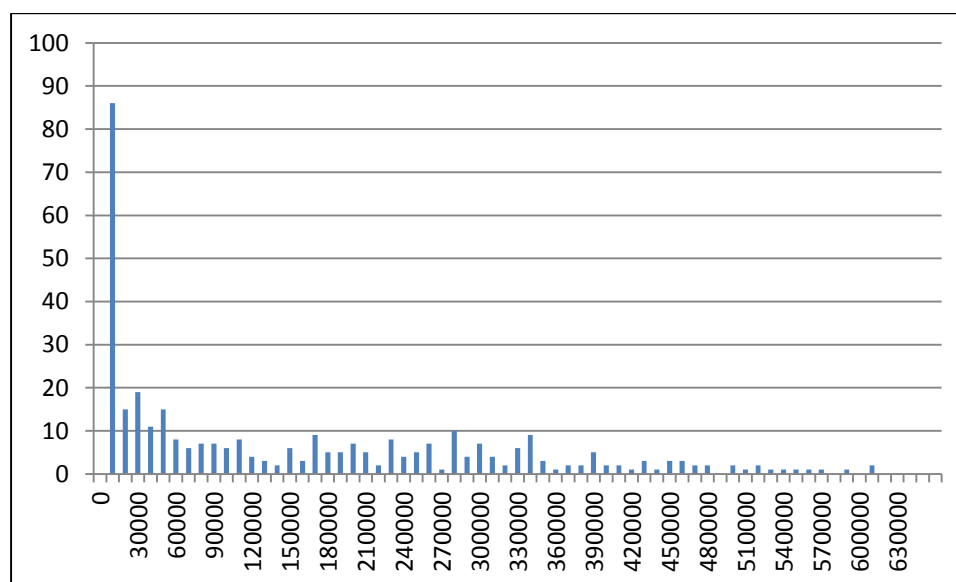
Figure 4. Frequency histogram of total lightning counts for 2009 showing the skewness of the data. The horizontal axis displays bins of lightning activity and the vertical axis show counts.

2010 lightning data review. This was the second most active year with 57,473,172 total strokes across the CONUS. Table 4 shows the lightning activity for each month broken into the four categories, and how much of the activity occurred during the summer. Again, very nearly two-thirds (66.61%) of lightning activity occurred during the summer months and the overwhelming majority, 90.67%, of recorded strokes were negative cloud-to-ground.

Table 5 contains a basic statistical analysis of the four lightning categories for 2010. The maximum events occurred on the following dates: total and negative were on August 5, 2010, positive was on May 24, 2010, and cloud-to-cloud was on July 14, 2010. The lightning event data distribution was again highly skewed (figure not shown).

Table 4

Monthly Lightning Activity for 2010

	% of Year	All Categories	Negative	Positive	Cloud-to-cloud
Jan	1.28%	737209	672061	15974	48946
Feb	0.72%	412466	374535	9507	28424
Mar	2.00%	1151824	1014013	32946	104865
Apr	4.56%	2623423	2320204	60503	242716
May	12.81%	7363147	6534138	161711	667298
Jun	22.37%	12854675	11670434	199936	984305
Jul	23.85%	13706851	12376036	208372	1122443
Aug	20.39%	11719448	10783410	129364	806674
Sep	7.26%	4173020	3855716	51163	266141
Oct	3.68%	2112453	1936036	29665	146752
Nov	0.77%	444646	412792	7705	24149
Dec	0.30%	174010	159261	4669	10080
Summer	66.61%	38280974	34829880	537672	2913422
Total		57473172	52108636	911743	4452793
% of all categories			90.67%	1.59%	7.75%

Table 5

Daily Lightning Statistics for 2010

	All Categories	Negative	Positive	Cloud-to-cloud
Maximum	733648	690514	14904	63268
Third Quartile	279666	253062	4017	19896
Mean	159205.5	144345.3	2525.604	12334.61
Median	76416	69391	1169	5566
First Quartile	8542	7449	218	542
Minimum (non-zero)	19	16	1	1
Standard Deviation	184818.1	168136.9	2954.774	14962.21
Interquartile Range	271124	245613	3799	19354

2011 lightning data review. This was the most active year with 58,077,226 total strokes across the CONUS. Table 6 shows the lightning activity for each month broken into the four categories, and how much of the activity occurred during the summer. Again, nearly two-thirds (62.17%) of lightning activity occurred during the summer months and the overwhelming majority, 90.59%, of recorded strokes were negative cloud-to-ground.

Table 7 contains a basic statistical analysis of the four lightning categories for 2011. The maximum events occurred on the following dates: total, negative and positive occurred August 1, 2011, and cloud-to-cloud was on July 20, 2011. The lightning event data distribution was again highly skewed (figure not shown).

Table 6

Monthly Lightning Activity for 2011

	% of Year	All Categories	Negative	Positive	Cloud-to-cloud
Jan	0.82%	474863	443605	10786	20252
Feb	0.70%	407507	348472	14835	44200
Mar	3.08%	1791578	1632496	36292	122790
Apr	7.73%	4487577	4043297	83663	360617
May	9.51%	5525819	4866601	120286	538932
Jun	16.83%	9776395	8747729	167261	861405
Jul	22.79%	13234443	11904092	227053	1103298
Aug	22.54%	13093146	12035358	194705	863083
Sep	10.51%	6103137	5695089	63706	344342
Oct	3.16%	1835142	1694643	30049	110450
Nov	1.87%	1083950	966129	20138	97683
Dec	0.45%	263669	234369	5943	23357
Summer	62.17%	36103984	32687179	589019	2827786
Total		58077226	52611880	974937	4490409
% of all categories			90.59%	1.68%	7.73%

Table 7

Daily Lightning Statistics for 2011

	All Categories	Negative	Positive	Cloud-to-cloud
Maximum	640343	544509	18239	79149
Third Quartile	284643	252524	4897	22364
Mean	159992.4	144936.3	2685.777	12370.27
Median	93654	85577	1423	5463
First Quartile	12264	10203	253.5	531
Minimum (non-zero)	3	3	1	2
Standard Deviation	168557.5	153028.1	2974.293	14326.55
Interquartile Range	272379	242321	4643.5	21833

Regional daily-sum event counts. Table 8 shows the sum of all stroke types at each spaceport for each year, the total for each spaceport for all three years, the percentage of lightning strokes that each spaceport contributed to the total of all spaceport events, and the percentage that each spaceport contributed to the total of all CONUS lightning strokes. The spaceports have been ranked based on the total lightning strokes over the three-year period, with CCS being the most active and CASP being the least active.

Table 8

Spaceports Ranked by Total Lightning Activity

	2009	2010	2011	Total	% of Spaceports	% of CONUS
CCS	573378	378184	526746	1478308	25.81%	0.88%
BAK	284555	514812	418872	1218239	21.27%	0.72%
CSM	357058	289424	257423	903905	15.78%	0.54%
SPAM	181619	211772	170694	564085	9.85%	0.34%
MARS	209454	150436	171360	531250	9.28%	0.32%
MHV	4680	18230	20581	43491	0.76%	0.03%
CASP	345	3883	5397	9265	0.17%	0.01%
Total	1,856,100	1,987,970	1,905,865	5,726,607		3.40%
CONUS	52,802,485	57,473,172	58,077,226	168,352,883		

The spaceports were grouped into three categories using linear bins based on total lightning activity at each spaceport over the three-year period. Spaceports with high activity are those with $\geq 988,627$ strokes, medium activity are those with $\geq 498,946$ but $< 988,627$ strokes, and low activity are those with $< 498,946$ strokes. Using this method, CCS and BAK are categorized with high activity. Spaceports categorized with medium activity are CSM, SPAM, and MARS. Spaceports categorized with low activity are MHV and CASP.

Characteristics of spaceports with high lightning activity. CCS and BAK had the greatest lightning activity of all spaceports analyzed. Both spaceports accounted for

47.08% of lightning activity at all spaceports analyzed and 1.6% of all lightning activity across the CONUS during the analysis period.

Monthly lightning activity for CCS is shown in Table 9 and the basic statistical analysis is shown in Table 10. CCS had the highest lightning activity of all spaceports analyzed, with a total activity of 1,478,308 events for all three years. Lightning events at CCS accounted for 25.81% of activity at spaceports and 0.89% of activity across the CONUS. During 2009 and 2011, 73.96% and 72.92% of lightning activity at CCS occurred during the summer (June, July, and August). In 2010, the lightning activity did not match the same summer pattern seen in 2009 and 2011, with only 49.33% of lightning activity occurring in the summer. This is the result of a considerably inactive July and a much more active May.

Table 9

Monthly Total Lightning Events for CCS

	2009		2010		2011		Total
	%	Strokes	%	Strokes	%	Strokes	
Jan	0.00%	6	1.79%	6779	1.26%	6661	13446
Feb	0.01%	29	0.74%	2810	0.00%	22	2861
Mar	0.05%	264	8.96%	33891	5.46%	28757	62912
Apr	2.55%	14616	4.35%	16453	4.17%	21953	53022
May	4.10%	23513	22.77%	86106	5.58%	29400	139019
Jun	17.98%	103071	28.67%	108443	18.87%	99390	310904
Jul	28.22%	161780	7.56%	28582	24.73%	130240	320602
Aug	27.77%	159230	13.10%	49533	29.32%	154458	363221
Sep	12.92%	74053	11.53%	43614	8.34%	43910	161577
Oct	4.76%	27289	0.47%	1782	2.21%	11638	40709
Nov	1.10%	6321	0.04%	133	0.00%	22	6476
Dec	0.56%	3206	0.02%	58	0.06%	295	3559
Summer	73.96%	424081	49.33%	186558	72.92%	384088	994727
Total		573378		378184		526746	1478308

The maximum daily number of lightning events at CCS occurred on the following days: on June 23, 2009, there were 30,883 events; on September 28, 2010, there were 22,050 events; and on July 15, 2011, there were 34,500 events. Each year had a consistent number of T-Storm Days (any day where at least one lighting stroke was

observed) with 184 in 2009, 177 in 2010, and 190 in 2011, totaling 551 T-Storm Days. The number of annual T-Storm Days statistically implies the following probabilities of a lightning stroke occurring on any given day during a particular year: 50.41% in 2009, 48.49% in 2010, and 52.05% in 2011. During the summer months (92 days from June 1 to August 31), the number of T-Storm Days was 90 in 2009, 86 in 2010, and 87 in 2011. Despite the notable reduction in lightning activity at CCS in the summer of 2010, there were still essentially the same number of T-Storm Days in 2010 as 2009 and 2011. Analysis was not conducted to determine how or why lightning activity was down but T-Storm Days remained the same. The probability of a lightning stroke occurring on any given summer day during a particular year was 97.83% in 2009, 93.48% in 2010, and 95.57% in 2011.

Table 10

Yearly Statistics of Total Lightning for CCS

	2009	2010	2011
Maximum	30883	22050	34500
Third Quartile	1497	313	1042
Mean	1633.56	1047.60	1451.09
Mean Non-zero	3116.19	2136.63	2772.35
Median	1	0	1
First Quartile	0	0	0
Standard Deviation	3660.74	2910.77	3569.98
Interquartile Range	1497	313	1042
T-Storm Days	184	177	190
Daily T-Storm Probability	50.41%	48.49%	52.05%
Summer T-Storm Days	90	86	87
Summer Daily T-Storm Probability	97.83%	93.48%	94.57%

Characteristics of spaceports with low lightning activity. Monthly lightning activity for CASP is shown in Table 11 and a basic statistical analysis is shown in Table 12. CASP had the lowest lightning activity of all the spaceports analyzed, with the total activity for 2009, 2010, and 2011 combined (9,625 events) less than monthly totals for many spaceports and even less than single days at CCS (on June 23, 2009, there were 30,883 recorded lightning events at CCS). CASP's lightning events accounted for 0.17% of activity at spaceports and 0.01% of activity across the CONUS. Lightning events at

CASP in September 2011 accounted for 96.16% of activity in 2011. September 2011 also accounted for 53.29% of lightning activity at CASP during all three years with 5,190 events. This activity was concentrated on September 10th and 11th with 2,120 events for 39.28% of annual activity, and 2,439 events for 45.19%, respectively. Other highly active events included May 2009 with 38.26% of annual activity, and October 2010 with 50.42% of annual activity.

Table 11

Monthly Total Lightning Events for CASP

	2009		2010		2011		Total
	%	Strokes	%	Strokes	%	Strokes	
Jan	0.87%	3	10.30%	400	0.00%	0	403
Feb	11.88%	41	1.21%	47	1.33%	72	160
Mar	1.16%	4	0.18%	7	0.22%	12	23
Apr	16.23%	56	0.03%	1	0.26%	14	71
May	38.26%	132	0.00%	0	0.54%	29	161
Jun	0.00%	0	0.00%	0	0.00%	0	0
Jul	0.00%	0	35.95%	1396	0.26%	14	1410
Aug	9.86%	34	0.00%	0	0.00%	0	34
Sep	0.00%	0	0.31%	12	96.16%	5190	5202
Oct	0.00%	0	50.42%	1958	0.04%	2	1960
Nov	0.29%	1	0.54%	21	1.00%	54	76
Dec	21.45%	74	1.06%	41	0.19%	10	125
Summer	9.86%	34	35.95%	1396	0.26%	14	1444
Total		345		3883		5397	9625

The maximum number of lightning events at CASP occurred on the following days: on December 12, 2009, there were 56 events; on July 11, 2010, there were 1,392 events; and on September 11, 2011, there were 2,439 events. Each year saw less than 30 T-Storm Days, with single highly active events changing the weight of an entire month.

Table 12

Yearly Statistics of Total Lightning for CASP

	2009	2010	2011
Maximum	56	1392	2439
Third Quartile	0	0	0
Mean	0.945205	10.63836	14.7863
Mean Non-zero	11.89655	143.8148	234.6522
Median	0	0	0
First Quartile	0	0	0
Standard Deviation	5.183157	85.92915	171.264
Interquartile Range	0	0	0
T-Storm Days	29	27	23
Daily T-Storm Probabilities	7.95%	7.40%	6.30%
Summer T-Storm Days	5	2	3
Summer Daily T-Storm Probabilities	5.43%	2.17%	3.26%

Brief Examination of CIP and Lightning Correlations

By reviewing the CIP and lightning data together, areas were found where lightning occurred with little or no CIP coverage. This is of particular concern since the CIP uses NLDN data to diagnose convective icing, but not extensively enough for all lightning activity to activate the CIP. Figures 5 and 6 show correlations between maximum CIP values and total flash counts on May 24, 2010 and May 25, 2010. Areas with no shading denote regions that contain no lightning, no CIP, or neither lightning nor CIP. Yellows, reds, and purple represent areas of increasing positive correlations, indicating either increasing CIP with increasing lightning or decreasing CIP with decreasing lightning. Shades of blue represent areas of negative correlations, indicating either decreasing CIP with increasing lightning, or increasing CIP with decreasing lightning. During the analysis, there were frequent instances of negative correlations observed. These results are critically important because they represent conditions where CIP fails to capture the true lightning hazard. In this first case, the areas of interest are Quebec and Ontario for multiple reasons.
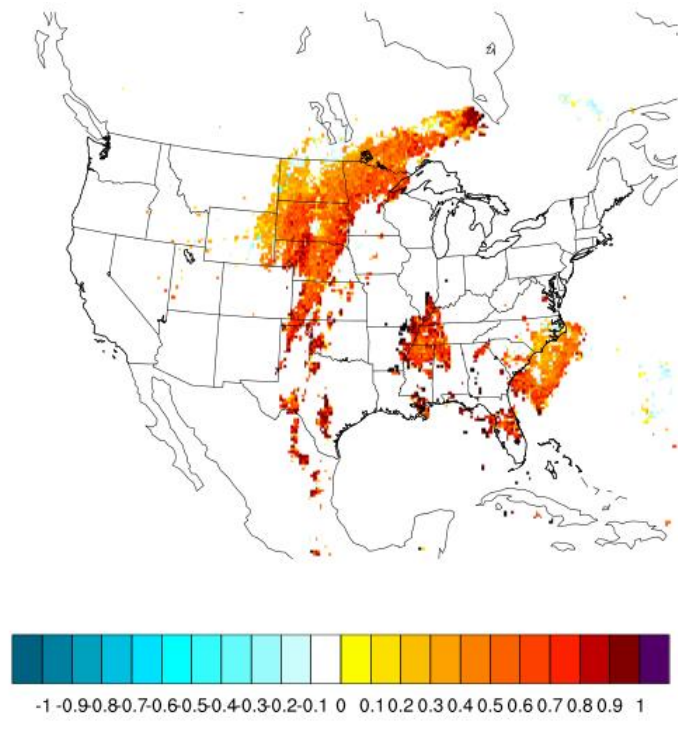
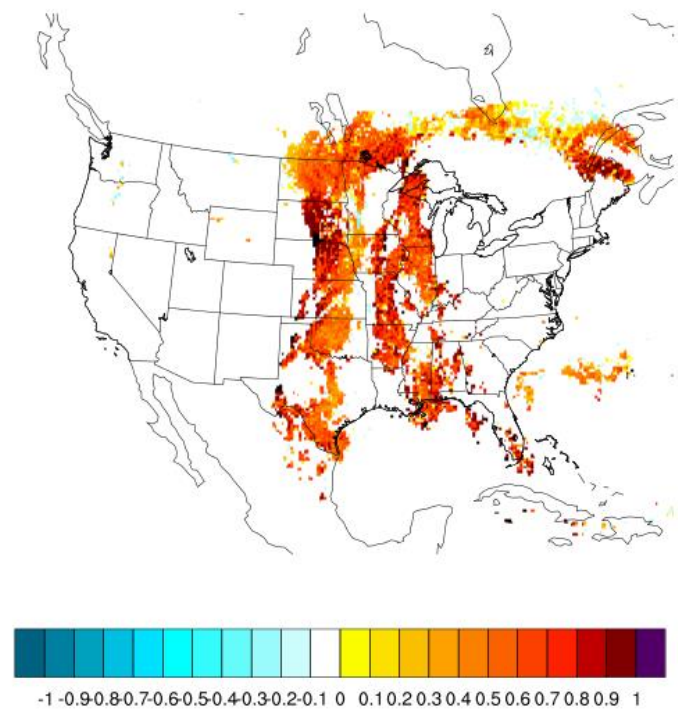*Figure 5*. Lightning and maximum CIP correlations for the CONUS on May 24, 2010.

Figure 6. Lightning and maximum CIP correlations for the CONUS on May 25, 2010.

Figure 7 is a display showing maximum CIP and lightning over the northeastern

U.S. and Canada on the same day as the correlations from Figure 5. CIP is colored using

the same scheme as the operational CIP with blues and greens denoting lower

probabilities of icing, increasing to yellows and reds for higher probability values.

Lightning uses a linear scaling from one stroke (black) blending into 366 strokes (blue).

The CIP has a partial transparency so the lightning data or the CIP is not covered by the

other data source. The result is that when lightning activity overlaps CIP the lightning

data will darken the CIP fields and add blue in cases of high lightning activity. An

example of the latter result in Figure 7 occurs in eastern North Dakota, where high

lightning activity (blue) and high CIP probabilities (red) generate purple as a new color
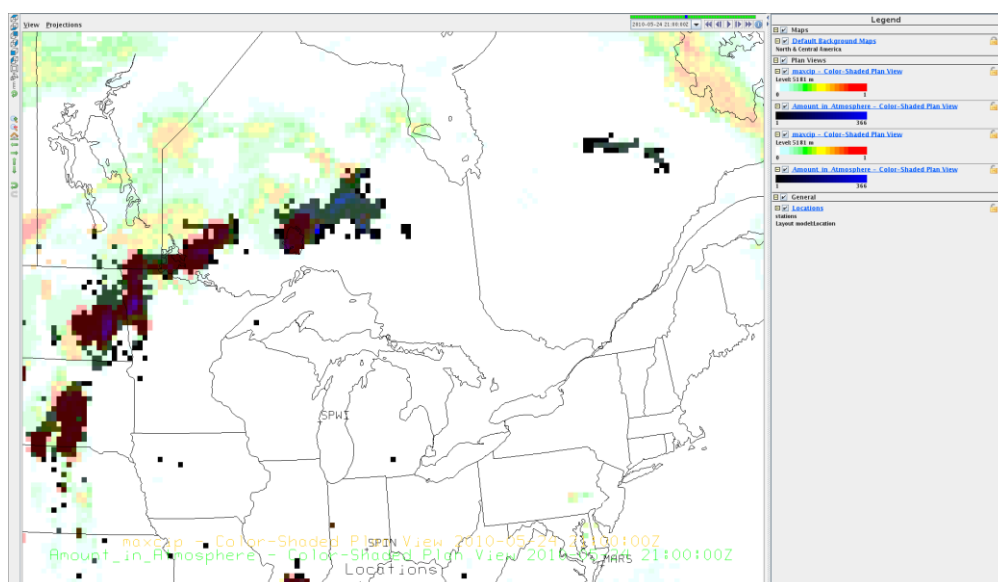
not used on either of the scales.

Figure 7. Intense lightning activity collocated with low CIP probabilities in Ontario and Quebec on May 24, 2010 at 21:00 UTC.

The area of lightning activity in Quebec initiated on May 24, 2010, at 20:00 UTC and moved east towards New Brunswick through May 25, 2010. In this case, the area of light lighting activity initiated with very low CIP probabilities that also lacked spatial coverage. Detailed analysis at 21:00 UTC, when the lightning activity began to increase, showed 38 grid boxes with lightning activity, 33 grid boxes with CIP probabilities (all less than 40% and most less than 25%), and 18 grid boxes where the data sets overlapped. As the lightning activity continued to increase, up to 169 strokes per hour in one grid box, the CIP probabilities began to match the activity better spatially, but the probabilities remained less than 40% until the hour after the 169-stroke event, when the CIP probability values jumped to 80% or greater. This jump was most likely due to the NLDN observations of lightning in that area prompting an increase in CIP values.

Another area of lightning, this one much more active, developed in the Central Plains early on May 24, 2010, and moved northeast into Ontario. Throughout the day, until 19:00 UTC, the lightning activity and high CIP probabilities (greater than 80%) were almost identically matched spatially. After 19:00 UTC, lightning activity began to extend beyond the high CIP probabilities until 04:00 UTC on May 25, 2010. By this time, more than half of the lightning activity was detached from the CIP probabilities, as shown in Figure 8. In addition, the grid boxes that still had CIP probabilities in proximity to the lightning activity had decreased significantly to less than 40%. To the north, away from the lightning activity, CIP probabilities remained high at greater than 80%. In this example, a combination of missed events and false alarms within the same synoptic-scale feature was observed.
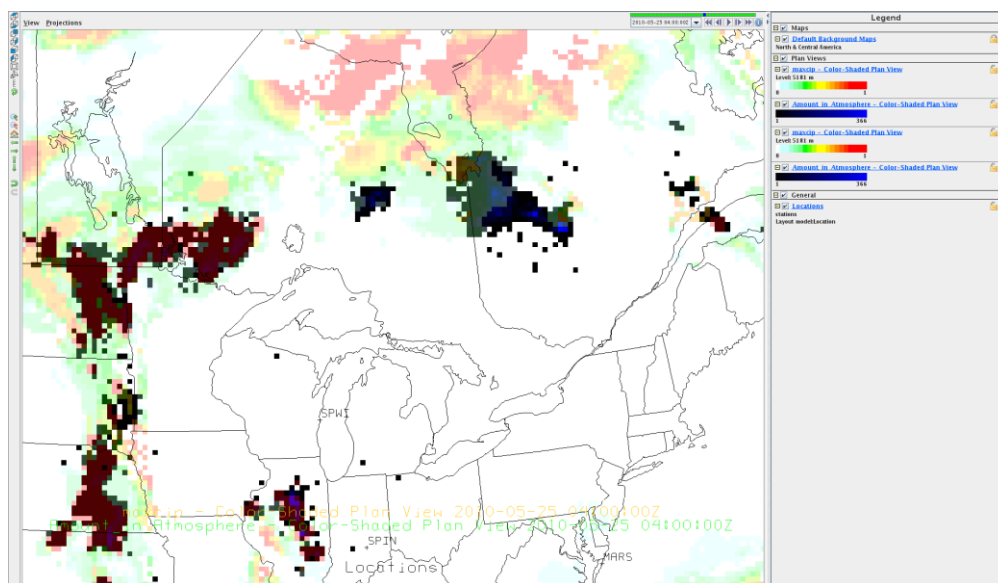
Figure 8. Intense lightning activity not being captured by CIP in Quebec on May 25, 2010 at 04:00 UTC; very high CIP probabilities with no lightning activity are just to the north.

CIP – Lightning Forecast Verification Results

Forecast verification scores for the CIP's ability to predict lightning were determined by building contingency tables. To provide a benchmark for comparison, forecast verification scores using contingency tables of observed lightning and lightning persistence forecasts were also generated. For additional comparison, forecast verification done by AMU at KSC is also included. Table 13 combines the location-specific contingency tables to show the CIP verification results for the seven active spaceports for 2009 and 2010. Most spaceports had very similar results between the number of Hits, Misses, False Alarms, and Correct Nulls. There were usually more Hits than Misses; in most cases, there were two to three times more hits. Spaceports where

this was not the case include MARS in 2009 where Missed events exceeded Hits, while

MHV and CASP in 2009 had very small numbers for both Hits and Misses, of similar

magnitudes.

While the relative magnitudes of Hits and Misses looks favorable for CIP as a

lightning predictor, the False Alarm events far exceeded Hits and Misses. For all

locations, the frequencies of False Alarms were several times greater than both the Hits

and Misses, and in some cases orders of magnitude greater. It would be possible to

reduce the False Alarm rate by increasing the threshold of CIP to something greater than

50%; however, doing this would increase the percentage of Misses. The problem with

Misses is discussed in more detail in the case study section below, where lightning occurs

with CIP values below the 50% threshold, along with other areas of False Alarms.

Table 13

CIP-Lightning Forecast Contingency Table Results for Spaceports

		Forecast			
		2009		2010	
Spaceport	Observed	Yes	No	Yes	No
Site	Yes	Hit	Miss	Hit	Miss
	No	False Alarm	Correct Null	False Alarm	Correct Null
BAK	Yes	8344	2659	8641	3092
	No	176247	803014	118006	683381
CASP	Yes	58	59	420	146
	No	37860	952287	39149	773405
CCS	Yes	10745	6835	8217	4281
	No	53047	919637	41470	759152
CSM	Yes	10216	2510	7616	2197
	No	69991	907547	67710	735597
MARS	Yes	6242	6835	3511	1427
	No	53047	919637	75864	732318
MHV	Yes	392	249	1325	360
	No	39819	949804	38599	772836
SPAM	Yes	7390	2696	8908	3643
	No	59604	920574	48280	752289

There are many additional measures of forecast quality that can be determined

from the contingency tables. Tables 14 (2009) and 15 (2010) provide some of these

forecast quality measures as a way to determine objectively the value of CIP as a predictor of a lightning hazard.

The quantities presented are defined as:

P = predicted events (H+FA),

E = total events (H+M),

T = total cases (H+M+FA+C),

F = frequency of the event (H+M)/C

False Alarm Rate = FAR = M/(H+FA) = FA/P,

Success Ratio = SR= H/(H+FA) = H/P = 1-FAR,

Probability of Detection = POD = H/(H+M), and the

Critical Success Index =CSI = H/(H+M+FA).

The interpretation of the results can be simplified by recognizing that for POD, SR, and CSI, high values are better with a possible range of zero to one, while for the FAR, lower is better for the same range. Low SR is due to a strong overprediction of the event, while a low CSI is due to high number of Misses and/or False Alarms in the forecast. The results are also provided graphically in annual groupings for interpretation and comparison.

Table 14

CIP-Lightning Forecast Verification Results for 2009

	BAK	CASP	CCS	CSM	MARS	MHV	SPAM
P:	184591	37918	63792	80207	125776	40211	66994
E:	11003	117	17580	12726	8585	641	10086
T:	990264	990264	990264	990264	990264	990264	990264
F:	0.0111	0.0001	0.0178	0.0129	0.0087	0.0006	0.0102
POD:	0.7583	0.4957	0.6112	0.8028	0.7271	0.6115	0.7327
FAR:	0.9548	0.9985	0.8316	0.8726	0.9504	0.9903	0.8897
SR:	0.0452	0.0015	0.1684	0.1274	0.0496	0.0097	0.1103
CSI:	0.0446	0.0015	0.1521	0.1235	0.0487	0.0097	0.1060

Table 15

CIP-Lightning Forecast Verification Results for 2010

	BAK	CASP	CCS	CSM	MARS	MHV	SPAM
P:	126647	39569	49687	75326	79375	39924	57188
E:	11733	566	12498	9813	4938	1685	12551
T:	813120	813120	813120	813120	813120	813120	813120
F:	0.0144	0.0007	0.0154	0.0121	0.0061	0.0021	0.0154
POD:	0.7365	0.7420	0.6575	0.7761	0.7110	0.7864	0.7097
FAR:	0.9318	0.9894	0.8346	0.8989	0.9558	0.9668	0.8442
SR:	0.0682	0.0106	0.1654	0.1011	0.0442	0.0332	0.1558
CSI:	0.0666	0.0106	0.1523	0.0982	0.0435	0.0329	0.1464

False Alarm Rates and Success Ratios. FARs and SRs for the CIP forecast of

lightning from 2009 and 2010 are presented in Figure 9. When calculated using data

from the entire period, all spaceports measured FARs greater than 0.83. Spaceports with

lower lightning activity, such as CASP, had FARs that round to 1.0 when given two

significant figures (the actual value is 0.9985). Spaceports with higher lightning activity,

such as CCS, tended to have slightly lower FARs. The AMU's findings at CCAFS/KSC

in 2005 indicated that a wet-season persistence forecast had a FAR of 0.37 and their

forecast equations had a FAR of 0.33. Unfortunately, the AMU did not perform forecast

verification in the years this study analyzed.
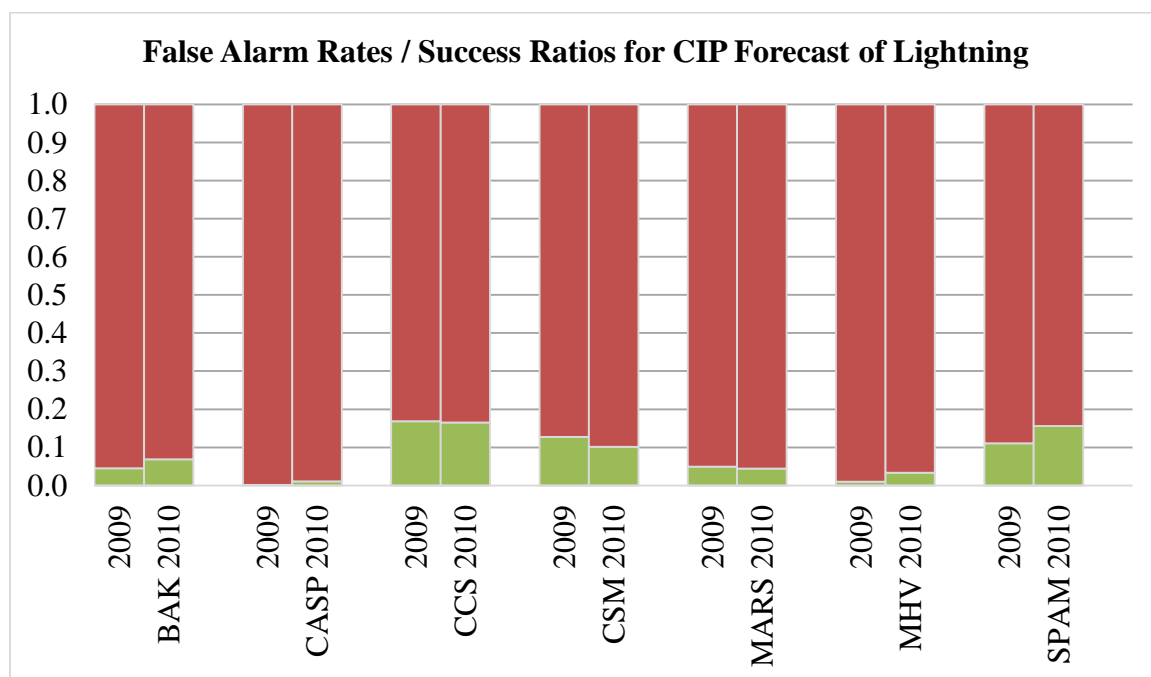
Figure 9. False Alarm Rates (red) and Success Ratio (green) for CIP forecast of
lightning in 2009 and 2010 at seven active spaceports.

Probability of Detection. Probabilities of detection (POD) for the CIP forecasts of lightning for 2009 and 2010 are presented in Figure 10. When calculated using data from the entire period, the POD seems to contradict the FAR. The POD is better than 0.50 for all spaceports, and better than 0.60 for all but CASP in 2009. In 2010, only CCS had a POD lower than 0.70. However, high POD can come from overprediction. POD does not penalize for how many total forecasts were made, and gross overprediction will inevitably capture more lightning events. Persistence forecasting at CCS in the wet season and the AMU's equation achieved similar PODs (0.67 and 0.75, respectively), but with much better performance in the other verification metrics, such as the FAR highlighted earlier (AMU, 2005).
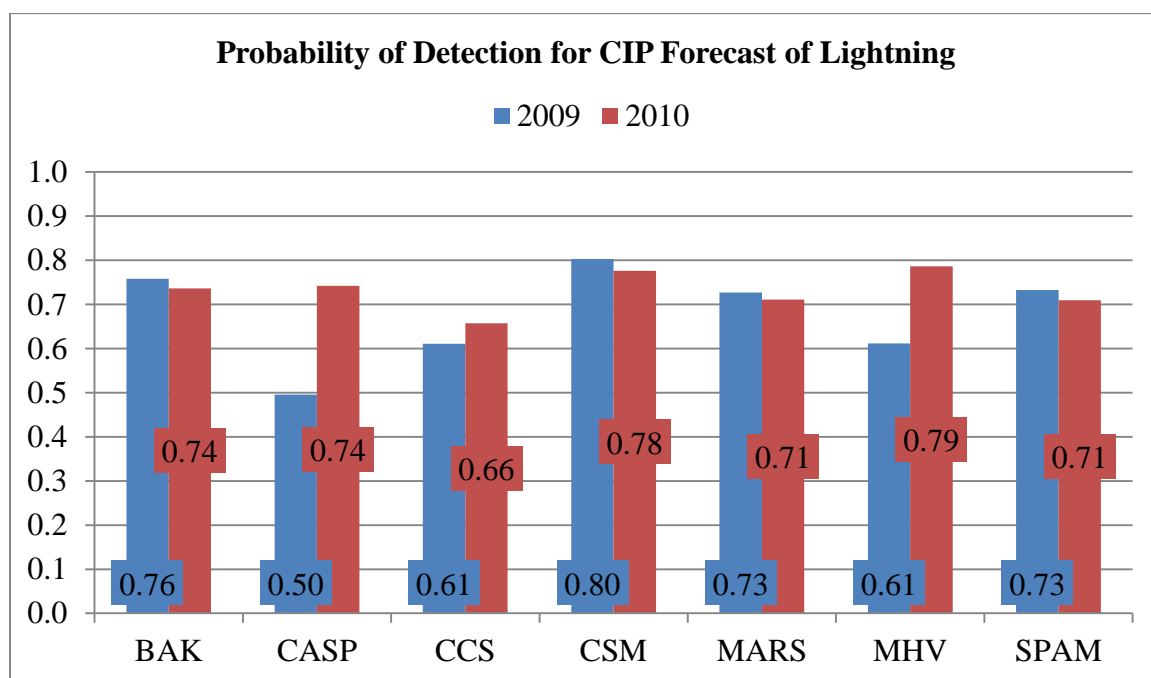
Figure 10. Probability of Detection rates for CIP forecast of lightning in 2009 (blue) and 2010 (red) for seven active spaceports.

Critical Success Index. The critical success index (CSI) scores for 2009 and 2010 are presented in Figures 11 and 12. Figure 12 provides a close up of Figure 11. When calculated using data from the entire two-year period, all spaceports have CSIs lower than 0.16. Spaceports with higher lightning activity managed better CSI scores than spaceports with lower lightning activity. CASP and MHV were less than 0.001 in 2009 and only slightly higher in 2010. By comparison, the AMU determined a wet-season persistence forecast at CCAFS/KCS had a CSI of 0.48, while their lightning forecast equations had a CSI of 0.55.
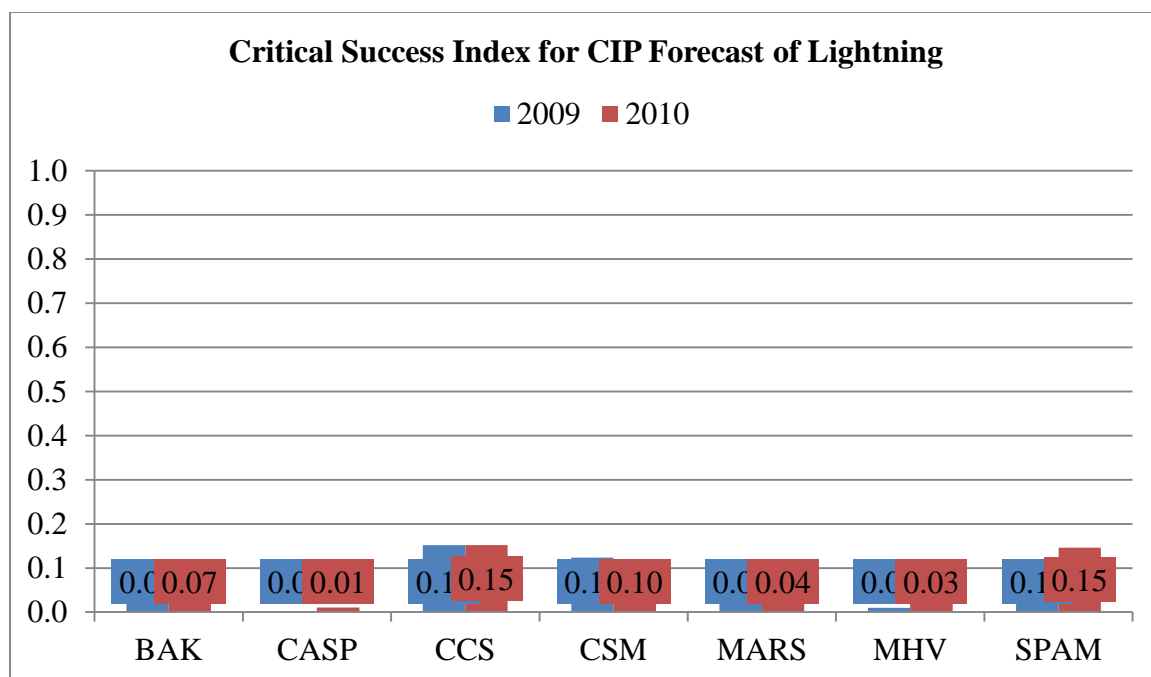
Figure 11. Critical Success Index scores for CIP forecast of lightning in 2009 (blue) and 2010 (red) at seven active spaceports.
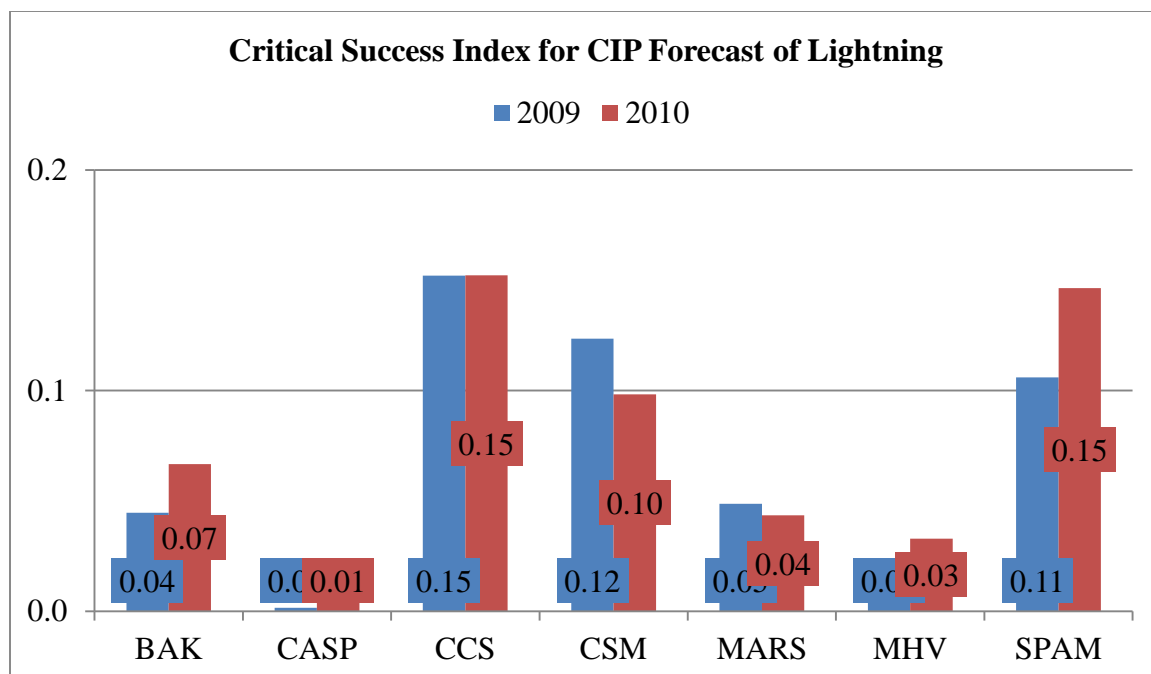
Figure 12. Close-up of Figure 11, showing Critical Success Index scores for CIP forecast of lightning in 2009 (blue) and 2010 (red) at seven active spaceports in more detail.

Persistence Forecast of Lightning Verification Results

Lighting persistence forecast verification was conducted from 2009 to 2011. The additional year of persistence verification was achieved because there were not the same gridding complications as with the CIP.

False Alarm Rates and Success Ratios. FAR and SR values for the lightning persistence forecast verification from 2009 to 2011 are presented in Figure 13. The FARs using lightning persistence as a forecast were substantially lower than using CIP as a forecast. Spaceports with more lightning activity, such as CCS and CSM, had lower FARs than spaceports with lower lightning activity, such as CASP.
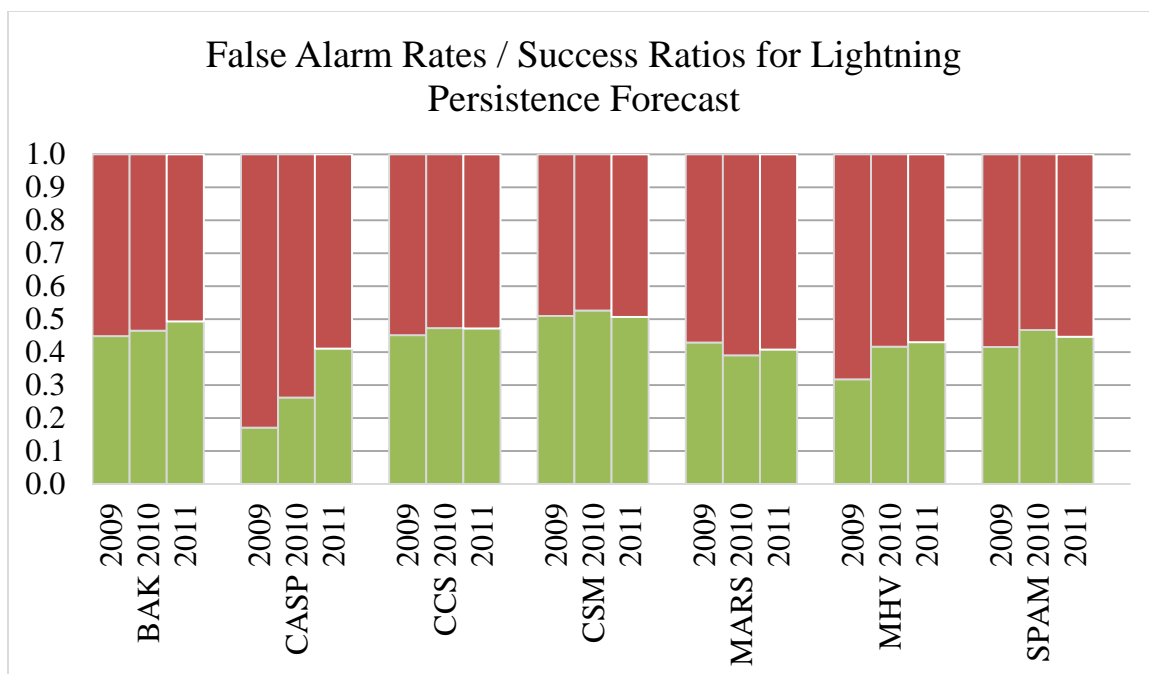
Figure 13. False Alarm Rates (red) and Success Ratio (green) for persistence forecast of lightning from 2009 to 2011 at seven spaceports.

Probability of Detection. POD for the lightning persistence forecast verification from 2009 to 2011 are presented in Figure 14. POD was consistent across all three years, with CASP and MHV (spaceports with "low lightning activity") having the most variability.

Critical Success Index. CSIs for the lightning persistence forecast verification from 2009 to 2011 are presented in Figure 15. Spaceports with higher lightning activity showed less variability between the three years analyzed than spaceports with less lightning activity. Spaceports with higher lightning activity also scored slightly better than spaceports with low activity. The CSI of most spaceports fell between 0.25 and 0.35.
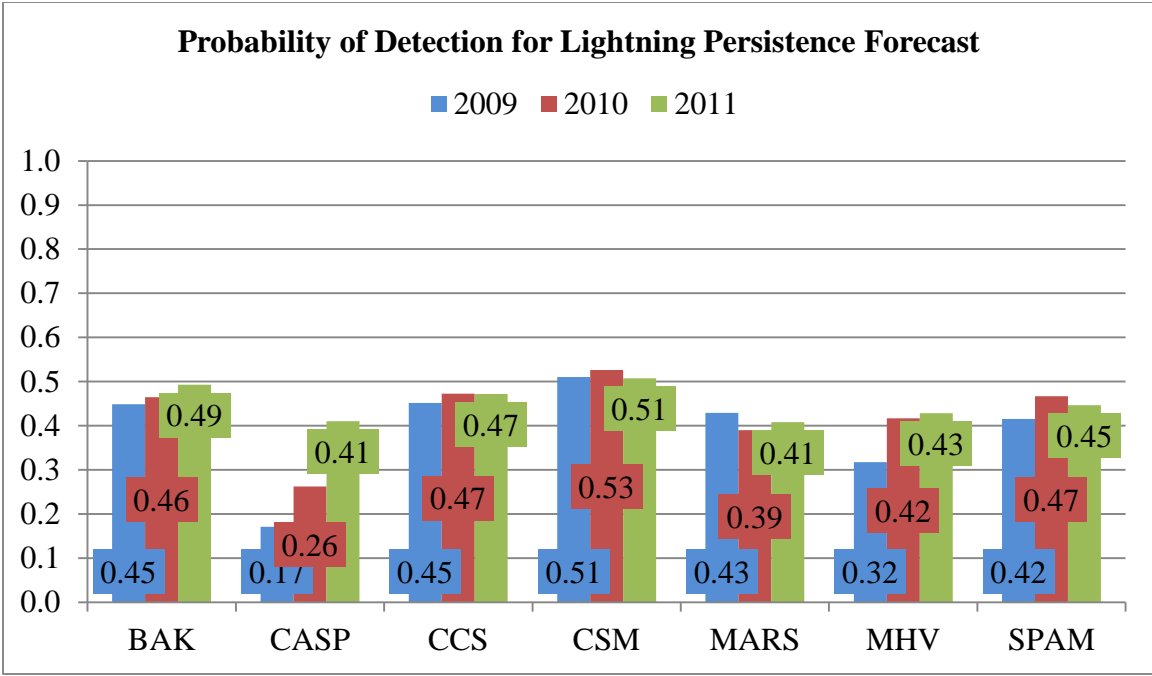
Figure 14. Probability of Detection rates for persistence forecast of lightning from 2009 to 2011 at seven spaceports.
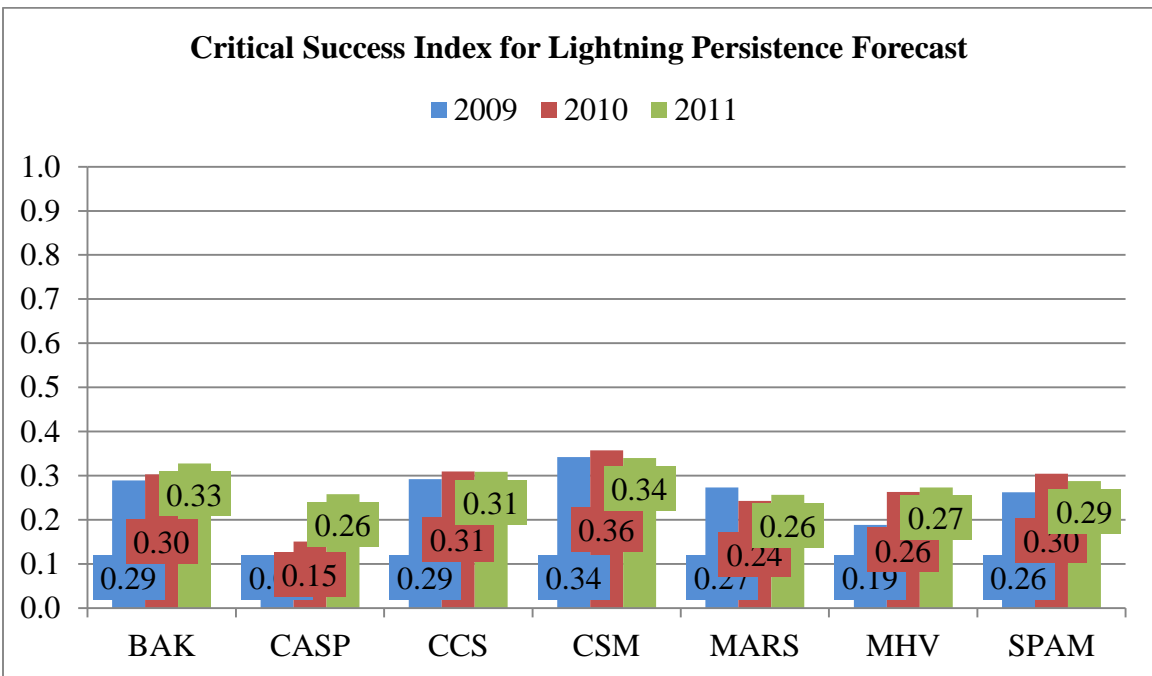

Figure 15. Critical Success Index scores for persistence forecast of lightning from 2009 to 2011 at seven spaceports.

Chapter V

Discussion, Conclusions, and Recommendations

During the literature review and initial statistical calculations, it was found that

the CIP uses NLDN lightning data as the primary source for identifying convective icing.

The 15 minutes of NLDN data prior to the valid time of the CIP are used as the primary

data for diagnosing convective icing hazards. Despite the inclusion of NLDN data in the

CIP, negative correlations between the CIP and USPLN were frequently found. These

results prompted further analysis and assessments to ascertain the CIP's ability to forecast

lightning. This additional analysis included forecast verification of the CIP and lightning,

verification of lightning persistence forecast, and case study analysis.

An analysis of lightning activity around selected spaceports demonstrated

relatively consistent seasonal variation in activity as well as the susceptibility of certain

spaceports to frequent lightning activity.

Discussion

Forecast verification. Though the POD of the CIP's lightning forecast is

reasonably high, this comes at the cost of a very high FAR. POD is calculated by taking

the number of Hits (H) and dividing by the sum of Hits and Misses (M). Because False

Alarms are not included in this method of calculating POD, a forecast system can make

unlimited positive forecasts without consequence (as long as there is at least one Hit).

Here is a simplified example: 10 hours of CIP values greater than 50% (the researcher's

threshold) exist at a single spaceport. Lightning only occurs on one hour during that

period. Table 16 shows the contingency table for this hypothetical situation, and the

forecast verification is calculated below the table.

Table 16

Contingency Table for Hypothetical CIP-Lightning Forecast Verification

		CIP ≥ 50%	
		Yes	No
	Yes	1	0
Lightning	No	9	0

$$P = Hits + False\ Alarms = 1 + 9 = 10$$

$$E = Hits + Misses = 1 + 0 = 1$$

$$T = Hits + Misses + False\ Alarms + Nulls = 1 + 0 + 9 + 0 = 10$$

$$F = \frac{E}{T} = \frac{Hits + Misses}{Hits + Misses + False\ Alarms + Nulls} = \frac{1}{1 + 0 + 9 + 0} = \frac{1}{10} = 0.10$$

$$POD = \frac{Hits}{E} = \frac{Hits}{Hits + Misses} = \frac{1}{1 + 0} = \frac{1}{1} = 1$$

$$FAR = \frac{False\ Alarms}{P} = \frac{False\ Alarms}{Hits + False\ Alarms} = \frac{9}{1 + 9} = \frac{9}{10} = 0.90$$

$$SR = \frac{Hits}{P} = \frac{Hits}{Hits + False\ Alarms} = \frac{1}{1 + 9} = \frac{1}{10} = 0.10$$

$$CSI = \frac{Hits}{P + E - Hits} = \frac{Hits}{Hits + Misses + False\ Alarms} = \frac{1}{1 + 0 + 9} = \frac{1}{10} = 0.10$$

This situation results in a POD of 100% because CIP predicted lightning (actually icing) every hour. The rest of the forecast verification metrics in this example (FAR, SR, and CSI) better reflect the very poor performance of this theoretical forecast. The SR and CSI are both only 10%. In fact, this hypothetical forecast designed specifically to

generate poor forecast verification has a *better* FAR than the actual CIP forecasts of lightning at BAK, CASP, MARS, and MHV. These four spaceports had FARs higher than 90%.

The CIP possesses less skill at forecasting lightning than a persistence forecast. The CIP's CSI at all spaceports was less than 0.20, and most were less than 0.10. Lightning persistence forecasts were better than CIP with CSIs higher than 0.20 for all spaceports except CASP and MHV in the western U.S. (which have few lightning days per year), and the rest nearing or exceeding 0.30. The lightning persistence forecasts performed better than the CIP despite being handicapped by the nature of persistence forecasts. Persistence will always verify a Miss on the first lightning strike and always verify a False Alarm after the last lightning strike. This means lighting activity lasting only one hour will result in two negative forecasts (Miss and False Alarm) and only one positive forecast (Hit). Lightning events lasting less than an hour will verify two negative forecasts. As such, persistence forecasts for lightning are mathematically unlikely to do better than 1/3, hence the more active spaceports nearing a 0.33 CSI.

Both CIP and lightning-persistence performed substantially worse than the AMU's lightning forecast tool at CCS[2], despite CCS having the best forecast verification scores for CIP and lightning-persistence. The AMU's tool surpassed both the CIP and persistence's PODs while maintaining a lower FAR than CIP and persistence. Development of this tool started with 13 predictors that were used in up to five different equations for forecasting wet season lightning probability. Some of these predictors included daily lightning climatology, persistence, flow regime lightning probability,

---

[2] The AMU's lightning forecast tool was developed using Florida wet season predictors to forecast wet season lightning.

Lifted Index, K-Index, Total Totals, and the Thompson Index. It might be possible to develop such equations for each individual spaceport, but such an exercise was beyond the scope of this study.

Lightning activity during analysis period. The analysis of CONUS lightning activity from the gridded data set showed relatively consistent seasonality between 2009, 2010, and 2011, with the winter months less active compared to peak activity in the summer months, as expected. Activity remained elevated during the spring and fall months, with some variation between the years and categories. Spaceports could be grouped into three categories based on the number of lightning strokes recorded over the course of the analysis period. Spaceports with high lightning counts experienced up to 200 T-Storm Days per year, while spaceports with low counts might see as few as three T-Storm Days a year. The variability in lightning activity demonstrates the need for detailed analysis of lightning hazards at each spaceport for individual risk assessment. For example, CCS has an extensive field mill network for lightning safety while VBG does not.

CIP and lightning correlations. The CIP was found to be highly correlated with lightning activity, likely because the CIP uses NLDN data to diagnose deep moist convection and convective icing hazards. Lightning flashes detected by the NLDN 15 minutes prior to the model valid time are assimilated into the CIP. The lightning is used as a predictor of a mixed-phase cloud, with strong updrafts, that will include supercooled liquid water. Despite the inclusion of NLDN data in the CIP, the CIP does not indicate all lightning activity, and analysis found negative correlations as well.

Conclusions

  Lightning poses a serious risk to operations and launch safety at commercial spaceports, though these risks are not equal across all spaceports. Using this study's parameters, some spaceports saw over one million lightning strokes per year while others experienced only a few thousand. Two previous incidents involving lightning strikes on launch vehicles have occurred, in one occasion resulting in the destruction of the vehicle. Experiments using instrumented aircraft flown in and around thunderstorms were able to conclude an aircraft (or spacecraft) is capable of triggering a lightning strike. Because of these findings and prior incidents, it is necessary for spaceports that operate in regions of frequent lightning activity to have tools for diagnosing lightning hazards. CCAFS/KSC, a government spaceport in an area of intense lightning activity, employs extensive lightning and atmospheric charge detection sensors, but commercial spaceports may not have such devices. If commercial spaceports cannot be mandated by government regulation to be equipped with the similar sensors, alternative diagnostic tools are necessary.

  This analysis has shown the CIP is not a suitable substitution for in-situ measurements of charged regions and dedicated lightning forecasting tools. Forecast verification showed the CIP would effectively generate a false lightning forecast 9 out of 10 times, or worse. The number of False Alarm forecasts for the two-year period analyzed were several orders of magnitude more than Hits and Misses combined. This makes CIP forecasts of lightning highly unreliable in an industry where incorrect forecasts are exceedingly expensive, not just for safety, but for scheduling and operations, as well.

The CIP was outperformed by persistence forecast of lightning, which itself is mathematically incapable of significantly exceeding a CSI of 0.33 for single cell thunderstorms with a life cycle of about an hour. These single cell, short-lived events present the most difficult forecast challenge and the greatest risk to safe operations. The only other operational lightning forecast system available for comparison during this study was a lightning forecast tool developed by the AMU at CCAFS. This tool significantly outperformed the CIP in all forecast verification metrics, including having a better POD with a lower FAR. This superior forecast methodology was achieved by using decades of meteorological data to select predictors for development of forecast equations, one equation for each month of the Florida wet season, specifically for CCAFS/KSC. Case study analysis showed the CIP largely over-predicts the extent of lightning and generally fails to capture both lightning initiation and cessation.

Recommendations

Neither the CIP nor the AMU's lightning forecast tool are capable of replacing lightning and charge detection devices for assessing the hazard of imminent lightning threats. Lightning detection, either by deployment of a dedicated network at commercial spaceports or subscription to commercially available lightning detection networks, is necessary for the assessment of current lightning activity. Field mills are necessary for the assessment of charge building up in the atmosphere, indicating lightning activity may be imminent. In addition to lightning detection equipment, lightning forecast tools must be developed for each commercial spaceport individually, using extensive climatological data for that area.

As numerical forecast systems gain higher resolution, storm formation is becoming a better-resolved part of the forecast. Where and when storms will form is a better diagnostic for lightning threat than looking for mixed water phase environments, humidity levels at various altitudes, or equations used to parameterize lightning formation[3]. Continued development of models capable of fully resolving thunderstorms is essential to lightning forecasting, and possibly future prediction of charge separation.

There is also no information for determining the CIP's ability to diagnose triggered lightning hazards. Studies agree a vehicle passing through a charged region could trigger the lightning stroke, but there are only a handful of cases of this occurring. These few cases do not provide enough evidence to draw any conclusions about the environment in which a vehicle may trigger a lightning stroke. More studies of rocket plume conductivity and environmental charge sensitivity need to be conducted to address the volume of questions that remain. In fact, it is possible that some regions of high CIP are capable of supporting a triggered lightning event. Given the inability to diagnose this hazard from historical data, no assessment of this hazard can be made from this study.

---

[3] The AMU's lightning forecast tool does not parameterize lightning formation. It uses specifically developed equations to determine the probability of lightning occurrence for planning purposes.

References

AMU. (2005). *Objective Lightning Probability Forecasting for Kennedy Space Center and Cape Canaveral Air Force Station.* NASA.

Benjamin, S. G., Devenyi, D., Weygandt, S. S., Brundage, K. J., Brown, J. M., Grell, G. A., . . . Manikin, G. S. (2004). An Hourly Assimilation–Forecast Cycle: The RUC. *Monthly Weather Review*, Vol 132, 495-518.

Bernstein, B. C., McDonough, F., Politovich, M. K., Brown, B. G., Ratvasky, T. P., Miller, D. R., . . . Cunning, G. (2005). Current Icing Potential: Algorithm Description and Comparison with Aircraft Observations. *Journal of Applied Meteorology*, Vol 44, 969-986.

Bothwell, P. D. (2009). Development, Operational Use, and Evaluation of the Perfect Prog National Lightning Prediction System at the Storm Prediction Center. *Fourth Conference on the Meteorological Applications of Lightning Data.* Phoenix, Arizona: American Meteorological Society.

Christian, H. J., Mazur, V., Fisher, B. D., Ruhnke, L. H., Crouch, K., & Perala, R. P. (1989). The Atlas/Centaur Lightning Strike Incident. *Journal of Geophysical Research*, Vol 94, 13169-13177.

FAA. (2011). *2011 U.S. Commercial Space Transportation Developments and Concepts: Vehicles, Technologies and Spaceports.* Office of Commercial Space Transportation.

Fitzgerald, D. R. (1967). Probable Aircraft "Triggering" of Lightning in Certain Thunderstorms. *Monthly Weather Review*, Vol 95, 835-842.

Gremillion, M. S., & Orville, R. E. (1999). Thunderstorm Characteristics of Cloud-to-Ground Lightning at the Kennedy Space Center, Florida: A Study of Lightning Initiation Signatures as Indicated by the WSR-88D. *Weather and Forecasting*, Vol 14, 640-649.

Hondl, K. D., & Eilts, M. D. (1994). Doppler Radar Signatures of Developing Thunderstorms and Their Potential to Indicate the Onset of Cloud-to-Ground Lightning. *Monthly Weather Review*, Vol 122, 1818-1836.

Moreau, J.-P., Alliot, J.-C., & Mazur, V. (1992). Aircraft lightning initiation and interception from in situ electric measurements and fast video observations. *Journal of Geophysical Research*, Vol 97, 15903-15912.

Murphy, M. J., Holle, R. L., & Demetriades, N. W. (2008). Cloud-to-Ground Lightning Warnings Using Electric Field Mill and Lightning Observations. *20th International Lightning Detection Conference, 2nd International Lightning Meteorology Conference.* Tuscon, Arizona: Vaisala, Inc.

Newman, M. M., Stahmann, J. R., Robb, J. D., Lewis, E. A., Matin, S. G., & Zinn, S. V. (1967). Triggered Lightning Strokes at Very Close Range. *Journal of Geophysical Research*, Vol 72, 4761-4764.

NOAA. (2015, August 12). *Rapid Refesh*. Retrieved from Earth System Research Laboratory: http://rapidrefresh.noaa.gov/

NOAA. (n.d.). *Reading Grib Files*. Retrieved from Climate Prediction Center: http://www.cpc.ncep.noaa.gov/products/wesley/reading_grib.html

Pitts, F. L., Fisher, B. D., Mazur, V., & Perala, R. A. (1988). Aircraft jolts from lightning bolts (electronic systems protection). *IEEE Spectrum*, Vol 25, 34-38.

Reap, R. M. (1986). Evaluation of Cloud-to-Ground Lightning Data from the Western United States for the 1983–84 Summer Seasons. *Journal of Climate and Applied Meteorology*, Vol 25, 785-799.

Rustan, P. L. (1986). The Lightning Threat to Aerospace Vehicles. *Journal of Aircraft*, Vol 23, 62-67.

Shafer, P. E., & Fuelberg, H. E. (2006). A Statistical Procedure to Forecast Warm Season Lightning over Portions of the Florida Peninsula. *Weather and Forcasting*, Vol 21, 851-868.

Shafer, P. E., & Fuelberg, H. E. (2008). A Perfect Prognosis Scheme for Forecasting Warm-Season Lightning over Florida. *Monthly Weather Review*, Vol 136, 1817-1846.

Shelton-Mur, K., & Walterscheid, R. L. (2010). *Triggered Lightning Risk Assessment for Reusable Launch Vehicles at Four Regional Spaceports.* Washington, D.C.: Commercial Space Transportation Advisory Committee (COMSTAC).

Spaceport Systems International. (n.d.). *What We Do*. Retrieved from The California Spaceport: http://www.calspace.com/Home/What_We_Do.html

Uman, M. A. (2001). *The Lightning Discharge.* New York, NY: Dover Publications.

Uman, M. A. (2011). *Lightning.* New York, NY: Dover Publications.

Uman, M., & Rakov, V. (2003). The interaction of lightning with airborne vehicles. *Progress in Aerospace Sciences*, Vol 39, 61-81.

Unidata. (n.d.). *Lightning Data Available via the Unidata LDM/IDD*. Retrieved from Unidata: http://www.unidata.ucar.edu/data/lightning.html#uspln

USNO. (2016). *Systems of Time*. Retrieved from U.S. Naval Observatory.

Wilks, D. S. (2006). *Statistical Methods in the Atmospheric Sciences.* Academic Press.

Appendix

Case Studies

CCAFS July 9, 2009

  Investigation of July 9, 2009, near CCS was selected by reviewing correlation

analysis between the gridded lightning and CIP data sets. Figure A1 shows numerous

areas of low to negative correlations across North America, including Florida, the

Atlantic Ocean, and Gulf of Mexico. In this case study, a stationary front, as shown by

the surface analysis in Figure A2, was positioned across the north Gulf coast and the

Florida panhandle producing strong convection over central Florida and CCAFS.
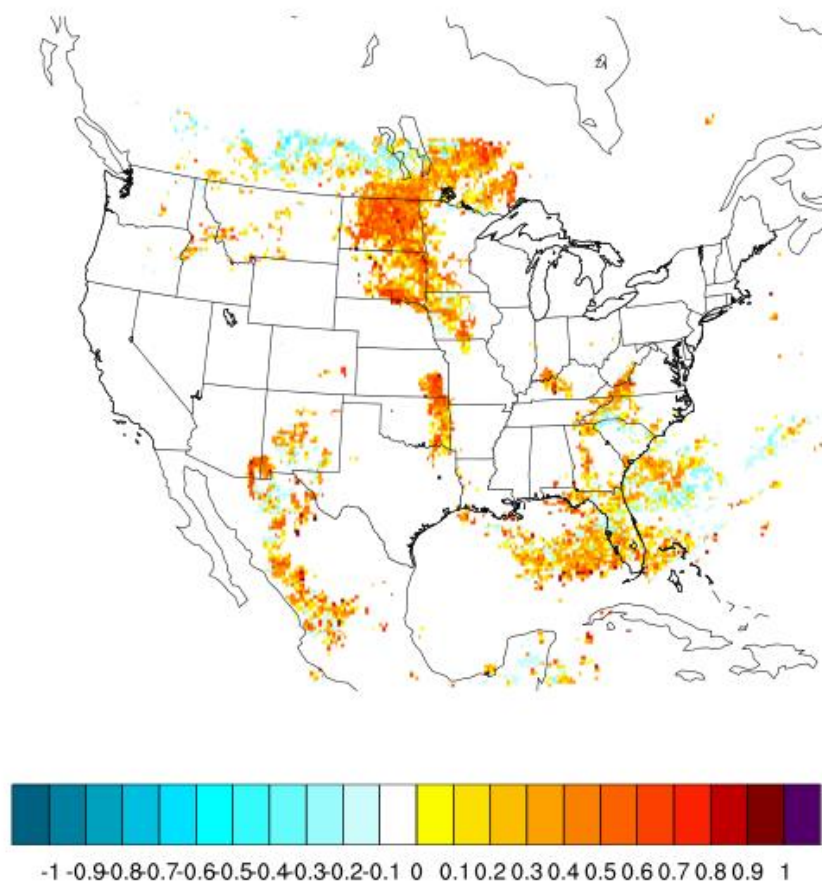
Figure A1. Lightning and maximum CIP correlations for the CONUS on July 9, 2009.
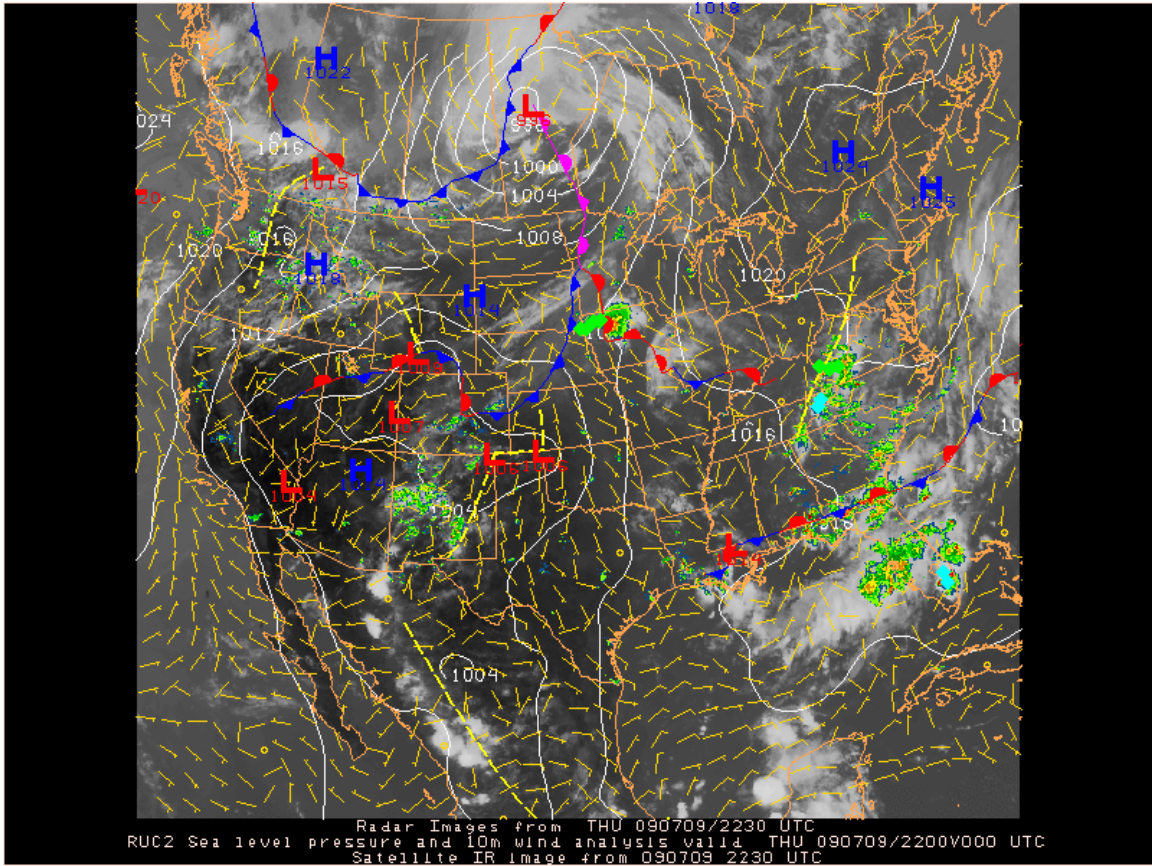
Figure A2. Surface analysis with satellite and radar imagery on July 9, 2009 at 22:30 UTC when lightning activity was closest to CCAFS.

The convection produced lightning throughout the day in the Gulf of Mexico, Florida, and the Atlantic with activity inside the regional domain for CCAFS most of the day. From 00:00 UTC to 07:00 UTC the CIP covered a very large portion of the CCAFS domain, particularly in the northwestern, northeastern, and southeastern quadrants as shown in Figure A3 (range rings at 50 km intervals centered over CCAFS have been added). This is contrast to the actual lightning activity, which is only in the southeastern quadrant for the first three hours before moving east into the Atlantic.
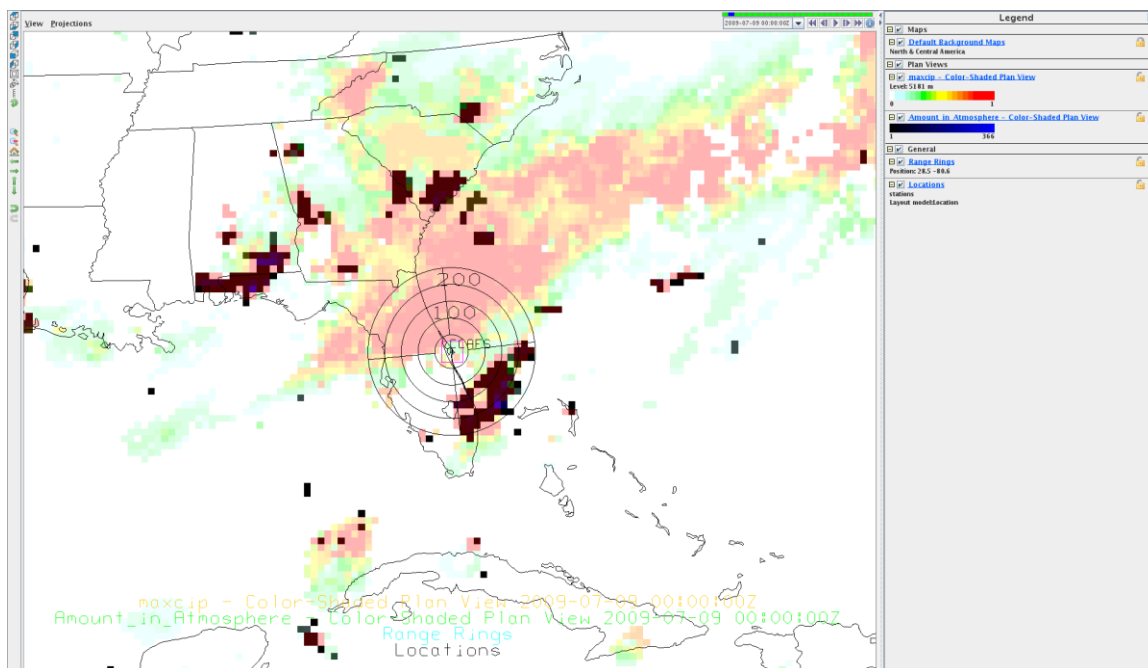
Figure A3. Very high CIP probabilities covering most of the CCAFS domain with lightning activity in only a quarter of the domain on July 9, 2009 at 00:00 UTC

By 11:00 UTC the large area of CIP probabilities had reduced back to well north and east of the CCAFS area, but in the northwestern quadrant a somewhat disorganized area of CIP probabilities was moving in from the Gulf of Mexico. Beyond that, there is some sporadic lightning activity and CIP probabilities in the Gulf of Mexico, shown in Figure A4. At 12:00 UTC, a large line of lightning activity initiates over the Gulf of Mexico in many areas there had previously been no CIP probabilities. The CIP fills in along this line with the lightning at the same time, shown in Figure A5.
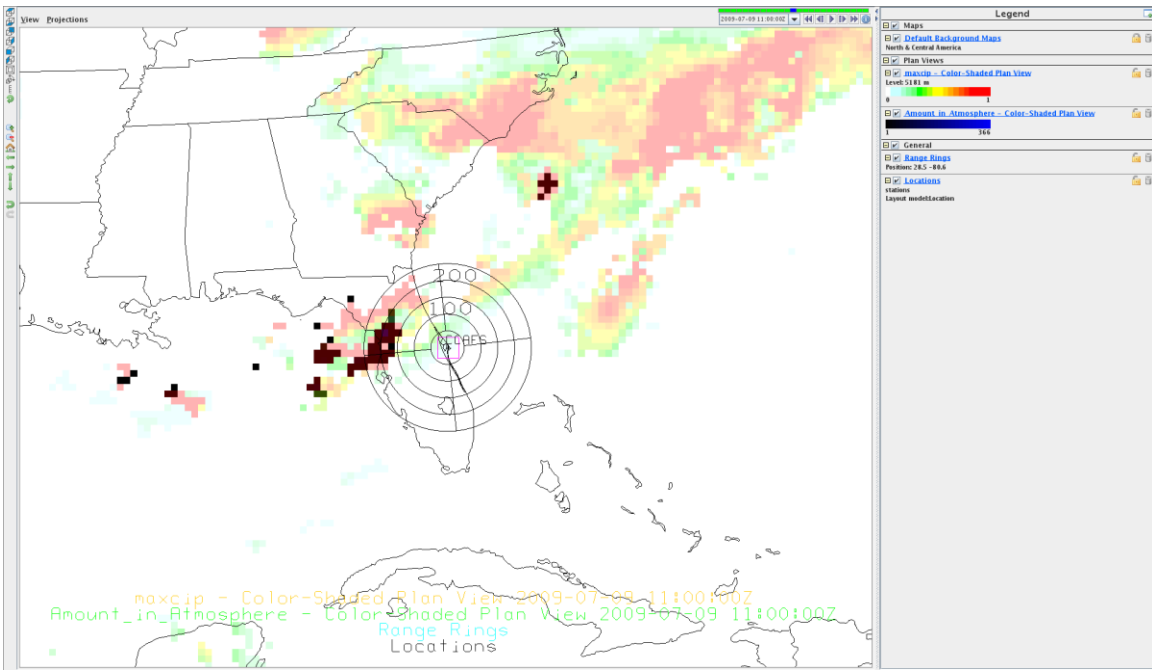
Figure A4. Unorganized CIP probabilities extending from western edge of CCAFS domain into the Gulf of Mexico on July 9, 2009 at 11:00 UTC
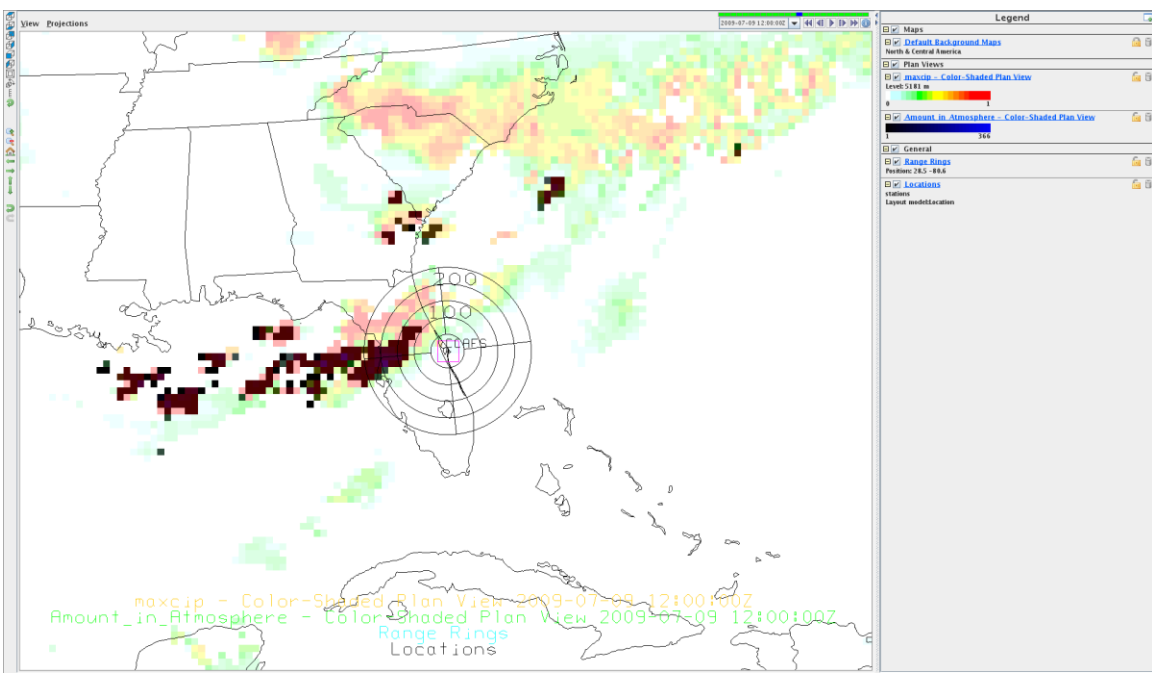

Figure A5. Lightning activity initiates in the Gulf of Mexico in areas where CIP probabilities had not existed the previous hour on July 9, 2009 at 12:00 UTC

SPAM March 8, 2010

In this case study an occluding low pressure system, as shown in Figure A6, was positioned over southern California moving east across Arizona into New Mexico. Convection started out light at 00:00 UTC on March 8, 2010, in proximity of the cold and occluded fronts wrapping into the center of the low with additional scattered convection in New Mexico. Quickly the convection in New Mexico intensified and by 01:50 UTC severe thunderstorm warnings were being issued for southeastern New Mexico that, among the hazards such as hail and damaging winds normally associated with severe thunderstorms, cautions of cloud to ground lightning were included in the warning issued by the NWS in Midland/Odessa, Texas:

```
WUUS54 KMAF 080150
SVRMAF
NMC015-080245-
/O.NEW.KMAF.SV.W.0001.100308T0150Z-100308T0245Z/
BULLETIN - EAS ACTIVATION REQUESTED
SEVERE THUNDERSTORM WARNING
NATIONAL WEATHER SERVICE MIDLAND/ODESSA TX
650 PM MST SUN MAR 7 2010
THE NATIONAL WEATHER SERVICE IN MIDLAND HAS ISSUED A
* SEVERE THUNDERSTORM WARNING FOR...
  CENTRAL EDDY COUNTY IN SOUTHEAST NEW MEXICO...
* UNTIL 745 PM MST
* AT 646 PM MST...NATIONAL WEATHER SERVICE METEOROLOGISTS
DETECTED A
  SEVERE THUNDERSTORM CAPABLE OF PRODUCING QUARTER SIZE
HAIL...AND
  DAMAGING WINDS IN EXCESS OF 60 MPH.  THIS STORM WAS LOCATED 9
MILES
  WEST NORTHWEST OF WHITES CITY...OR 20 MILES SOUTHWEST OF
  CARLSBAD...MOVING NORTHEAST AT 15 MPH.
* THE SEVERE THUNDERSTORM WILL AFFECT THE FOLLOWING LOCATIONS...
  CENTRAL EDDY COUNTY...
&&
LAT...LON 3272 10444 3258 10403 3213 10441 3219 10465
TIME...MOT...LOC 0149Z 207DEG 14KT 3224 10451
$$
```
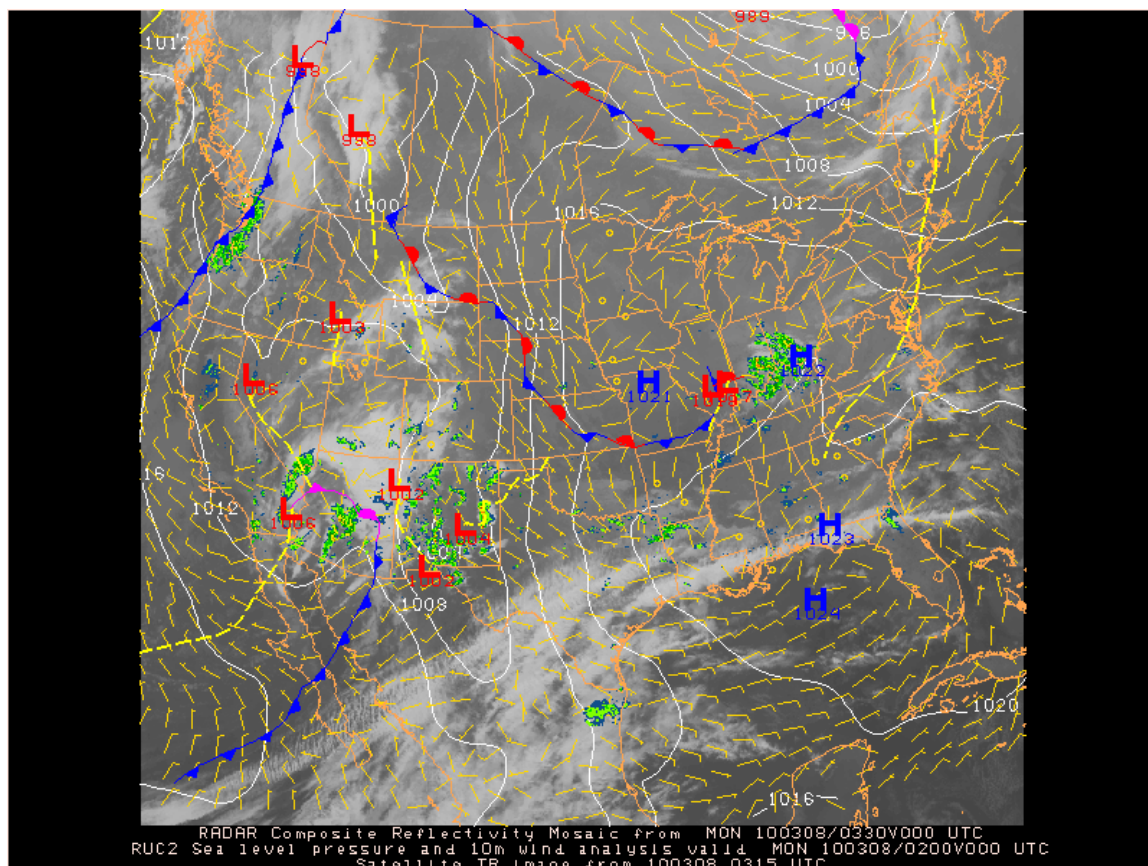
Figure A6. Surface analysis with satellite and radar imagery on March 8, 2010 at 03:15Z when lightning activity was closest to SPAM.

Lightning activity during the early hours of March 8 was low and located mostly in New Mexico including activity within the SPAM regional domain to the west, north, and east. The CIP probabilities were high in the northwest quadrant of the domain and low transition to high in the northeast domain as the distance from the spaceport increased. Figure A7 shows the initial lightning activity and CIP probabilities near SPAM as well as the rest of the southwestern and south central U.S., including a CASP, CSM, MHV, and Chugwater Spaceport (non-active). Note the large swath of high CIP probabilities in Texas, Oklahoma, Louisiana, and the Gulf of Mexico with no lightning activity.
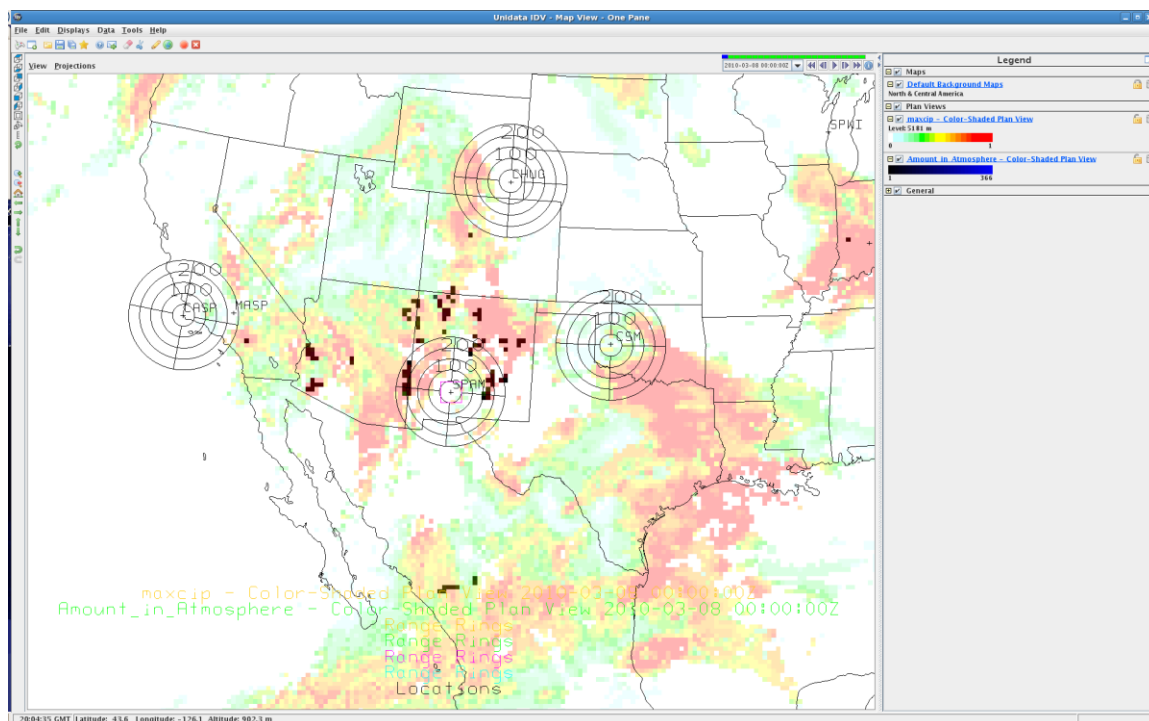
Figure A7. Initial lightning activity and CIP probabilities on March 8, 2010, over the southwestern and south central US including SPAM, CASP, CSM, and CHUG spaceports.

Until 04:00 UTC on March 8, 2010, CIP probabilities remained within the SPAM domain without probabilities higher than 75% (oranges) encroaching closer than about 100 km. Lightning activity continued to circle SPAM from west through north to east in a scattered manner until 02:00 UTC and 03:00 UTC when lightning activity was observed in the grids adjacent to and including SPAM. Figure A8 shows the progression of this lightning activity and the behavior of the CIP probabilities.
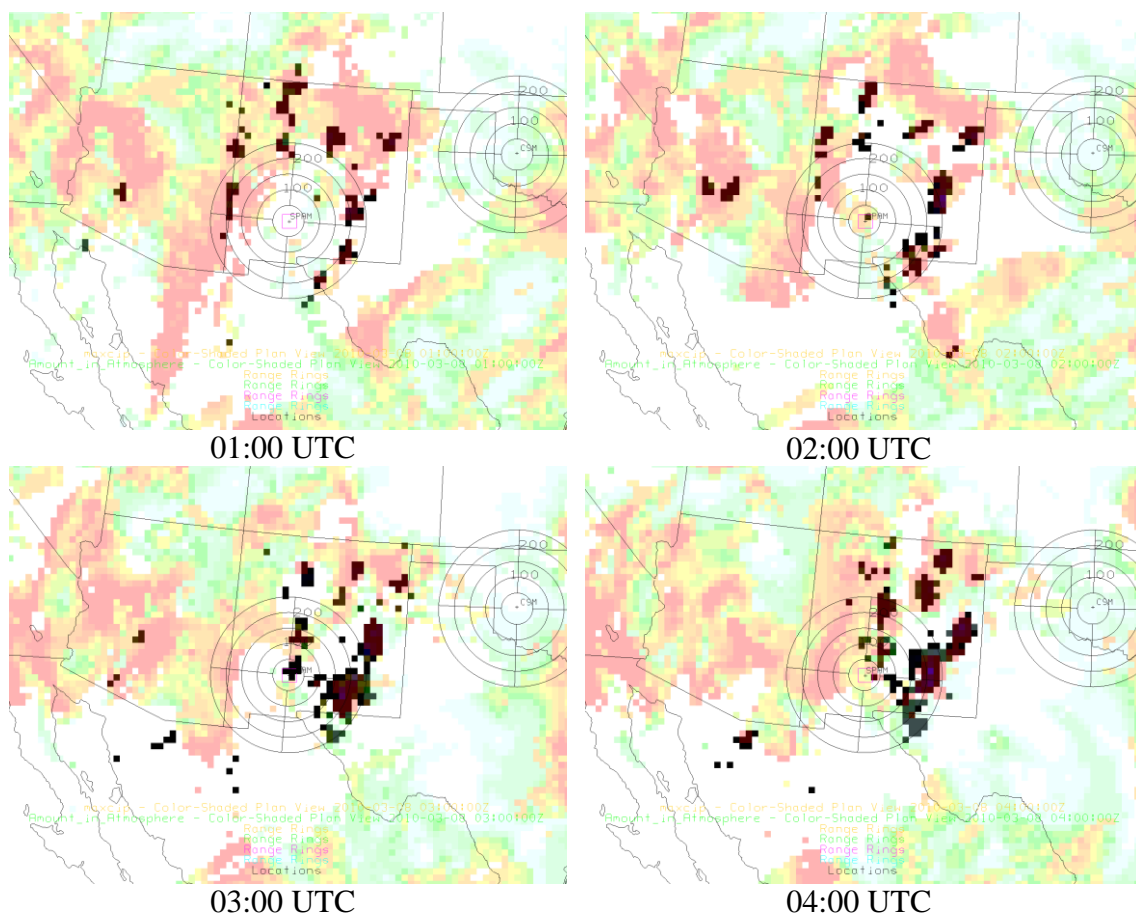
Figure A8. Sequence of lightning activity and CIP probabilities on March 8, 2010, starting at 01:00 UTC and ending at 04:00 UTC.

Intense lightning activity also initiated in the southeast quadrant of the SPAM domain. The lightning activity in the direct vicinity of SPAM and in the southeast domain quadrant developed in regions where CIP probabilities were either much lower or non-existent in the proceeding hours, especially when compared to the high background CIP probabilities in Arizona, Mexico, and California where little to no lightning activity occurred. In particular, the lightning activity over SPAM at 03:00 UTC initiated with only a few grid boxes within 50 km of the spaceport indicating low to moderate CIP probabilities and none indicating high probabilities. During this period even greater

lightning activity initiated in the southeast quadrant of the SPAM regional domain in

areas where CIP probabilities lower and more sparse than in other quadrants such as the

northwest and southwest.